



RESEARCH ARTICLE

10.1029/2022EA002541

Key Points:

- The study provides information on the prevailing transport and (re)deposition mechanisms in Lake Issyk Kul today
- Geochemical, granulometric, lipid biomarker, diatom, and statistical analyses were performed on surface sediment and inlet stream samples
- The results are prerequisite to interpret longer sediment successions from the lake

Supporting Information:

Supporting Information may be found in the online version of this article.

Correspondence to:

B. Wagner,
wagnerb@uni-koeln.de

Citation:

Lenz, M. M., Scheuer, R., Zhang, X., Jaeschke, A., Opitz, S., Leicher, N., et al. (2023). Modern sedimentation patterns in Lake Issyk Kul (Kyrgyzstan), derived from surface sediment and inlet stream samples. *Earth and Space Science*, 10, e2022EA002541. <https://doi.org/10.1029/2022EA002541>

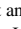



Received 11 OCT 2022

Accepted 15 AUG 2023

Author Contributions:

Conceptualization: X. Zhang, A. Jaeschke, B. Wagner
Data curation: M. M. Lenz, E. Rahmedinov, V. Wennrich, B. Wagner
Formal analysis: M. M. Lenz, R. Scheuer, X. Zhang, A. Jaeschke, S. Opitz, M. Pöllen, X. Xu, V. Wennrich
Funding acquisition: B. Wagner
Investigation: M. M. Lenz, R. Scheuer, X. Zhang, A. Jaeschke, S. Opitz, N. Leicher, M. Pöllen, X. Xu, V. Wennrich, B. Wagner

Modern Sedimentation Patterns in Lake Issyk Kul (Kyrgyzstan), Derived From Surface Sediment and Inlet Stream Samples

M. M. Lenz¹ , R. Scheuer¹, X. Zhang², A. Jaeschke¹, S. Opitz³, N. Leicher¹ , M. Pöllen¹, X. Xu², J. Rethemeyer¹, E. Rahmedinov⁴, K. Abdrakhmatov⁴, V. Wennrich¹ , and B. Wagner¹ 

¹Institute of Geology and Mineralogy, University of Cologne, Cologne, Germany, ²Institute of Loess Plateau, Shanxi University, Taiyuan, China, ³Institute of Geography, University of Cologne, Cologne, Germany, ⁴Institute of Seismology, National Academy of Sciences of Kyrgyz Republic, Bishkek, Kyrgyzstan

Abstract This study provides a descriptive characterization of the modern sedimentary processes in Lake Issyk Kul, Kyrgyzstan, important for the selection of a suitable coring or deep-drilling site, interpretation of future core data and applicability of proxies. The quasi-equidistant sampling grid of 66 sediment surface samples covers the entirety of the lake basin and is complemented by 10 samples from the major inflows. The methodological approach includes geochemical, granulometric, lipid biomarker, diatom, and statistical analyses. The quantitative and qualitative changes in sediment composition yield information on its generic origin and prevailing transport and depositional environments. The composition of the surface sediments in Issyk Kul is highly heterogeneous. Nearshore deposition is mainly controlled by wave action and by fluvial sediment supply with highest quantities of detrital input coming from the high-energetic, eastern tributaries. Sediments in the deep central basin are mainly produced in situ and dominated by authigenic calcite. Biogenic accumulation is overall low, except for the western extremity of the lake, where the nearshore, shallow-water, and low-energetic environment favors aquatic productivity and subsequent preservation of organic material and diatoms. Redeposition of sediments is a dominant process along the slopes across the southern and western basin floor, where run-out distances of mass movement deposits are up to 5 km. Directional sediment transport by lake currents appears to be less important, except for the transport of very fine-grained organic matter. Biomarker-inferred temperature reconstructions suggest lake surface temperatures of ~15°C in the western littoral zone and in Tyup Bay and a decrease to ~13°C basinward.

Plain Language Summary Intensive research on the natural component of climate variability on geological time scales is needed to better understand and validate current and future climate change. Lakes can provide continuous sediment successions that allow us to reconstruct regional trends in climate and environment dynamics far beyond the industrial age. In continental Eurasia, Lake Issyk Kul, one of the deepest and largest mountain lakes in the world, has long been targeted for a deep-drilling campaign, because its sediment succession potentially holds information of the past ~10 million years. Prerequisite for future drilling is a better understanding of prevailing transport and (re)deposition mechanisms in Lake Issyk Kul. The overarching aim of this study is to test the applicability of different proxies, vital for the interpretation of future sediment core data. Therefore, a quasi-equidistant sampling grid of up to 66 sediment surface (and 10 river) samples spanning the entire lake basin of Lake Issyk Kul was examined by means of sedimentological, geochemical, biological, and statistical analyses. The interpretation provides insights into spatial differences in, for example, clastic input from major rivers, biogenic sedimentation, and endogenic precipitation of calcium carbonates.

1. Introduction

Lake Issyk Kul (henceforward called Issyk Kul, since Kul means lake) is located in the heart of the Tien Shan Mountains, Central Asia and is one of the largest and deepest lakes worldwide. The lake archive is of great scientific interest, because the lake basin hosts a sediment succession up to 3,500 m thick, which potentially holds information on climatic trends and landscape development in continental Eurasia spanning the last ~10 million years (Shabunin & Shabunin, 2002). The intracontinental location of the lake offers an unique opportunity to study midlatitude climate change at a location marginally affected by changes in monsoons or marine conditions

© 2023 The Authors. Earth and Space Science published by Wiley Periodicals LLC on behalf of American Geophysical Union.

This is an open access article under the terms of the [Creative Commons Attribution License](https://creativecommons.org/licenses/by/4.0/), which permits use, distribution and reproduction in any medium, provided the original work is properly cited.

Methodology: M. M. Lenz, R. Scheuer, X. Zhang, A. Jaeschke, S. Opitz, N. Leicher, M. Pöllen, X. Xu, J. Rethemeyer, V. Wennrich

Project Administration: E. Rahmedinov, K. Abdrakhmatov, B. Wagner

Software: M. M. Lenz, V. Wennrich

Supervision: J. Rethemeyer, K.

Abdrakhmatov, B. Wagner

Validation: M. M. Lenz, E. Rahmedinov, V. Wennrich, B. Wagner

Visualization: M. M. Lenz, V. Wennrich

Writing – original draft: M. M. Lenz,

X. Zhang, A. Jaeschke, B. Wagner

Writing – review & editing: B. Wagner

(Oberhänsli & Molnar, 2012). Characteristics of Issyk Kul have been investigated within several fields of research providing data on, for example, the tectonic evolution (Roud et al., 2021), earthquake occurrence (Korzhenkov & Deev, 2017), seismic-stratigraphy (Gebhardt et al., 2017), geomorphology (Burgette et al., 2017; Rosenwinkel et al., 2017), recent climate (Shabunin & Shabunin, 2002), water chemistry (Karmanchuk, 2002), hydrobiology (Rojas-Jimenez et al., 2021; Romanovsky, 2002b; Savvaitova & Petr, 1992), hydrophysical characteristics (Romanovsky & Shabunin, 2002; Zavialov et al., 2020), and pollutants (Li et al., 2020, 2022; Liu et al., 2020).

Up to 5.2 m long gravity or piston cores have been collected from the lake, mostly from areas with a water depth of up to ~350 m and covering the Holocene with only a few older records (back to ~13 ka) (Leroy et al., 2021 and references therein). These cores yielded detailed insights into, for example, the paleolimnology and Holocene climate evolution (Ricketts et al., 2001), environmental and vegetation history (Giralt et al., 2002, 2004; Leroy et al., 2021; Zhang et al., 2021), hydrological regime (Wang et al., 2021), the sedimentary environment (De Batist et al., 2002), and paleomagnetic properties of the sediments (Gómez-Paccard et al., 2012; Larrasoaña et al., 2011). The potential of scientific deep-drilling in Issyk Kul has been widely discussed to obtain cores that provide a means to accurately reconstruct climate over several glacial cycles at a decadal to centennial resolution (Oberhänsli & Molnar, 2012; Zavialov et al., 2020). Deep-drilling will help to identify temporal variations in atmospheric circulation, moisture advection and insolation, evaluate the impact of tectonics and climate on erosion rates, test effects of abrupt climate changes and marine influences such as caused by Dansgaard-Oeschger stadials. Moreover, it may unravel the glaciation history of the Tien Shan mountains, provide a record of earthquake activity and trace the taxonomic diversity and evolution in the basin (Oberhänsli & Molnar, 2012).

In this context, to determine the most informative locations for prospective drilling, and correctly interpret the results, it is necessary to have a thorough understanding of the major sources of sedimentary material, transport mechanisms within the lake, early diagenetic processes and applicability of different proxies. Comparable studies have been successfully performed in preparation for other deep-drilling projects, for example, on surficial lake sediments from Lake Ohrid (North Macedonia/Albania; Vogel et al., 2010), Lake El'gygytgyn (Chukotka, Russia; Wennrich et al., 2013), Lake Towuti (Sulawesi, Indonesia; Hasberg et al., 2019), and Lake Van (Turkey; Reimer et al., 2009). Within the scope of this study, we processed 66 lake sediment surface samples from Issyk Kul and sediment samples from 10 river inlets to obtain crucial information on recent sedimentation characteristics and to disentangle the influence of climate, vegetation, water chemistry, different sediment sources, catchment and basin morphology, redeposition of sediments, lake internal transport as well as depositional and early diagenetic processes.

2. Study Area

Issyk Kul is an endorheic mountain lake in the Northern Tien Shan mountains in Eastern Kyrgyzstan (Figure 1). The lake is located at an elevation of 1,606 m above sea level (a.s.l.) and has an east-west and north-south extent of ~180 and ~60 km, respectively. The central, flat basin floor with a maximum water depth of 668 m occupies 25% of the lake area (Gebhardt et al., 2017). In its south-eastern part, a ~150 m high, ~20 km long, and ~4 km wide NE-SW elongated anticline emerges from the lake floor, gently dipping toward the southwest (De Batist et al., 2002; Figure 1). The eastern lake basin is shaped by two subaquatic gently dipping platforms (Figure 1). The upper, up to 110 m deep platform is incised by channels 50 m deep and up to 3 km wide, which represent submerged prolongations of the recent river mouths. The lower platform has a maximum water depth of ~340 m and is characterized by terraces representing ancient deltaic low stands (De Mol, 2006). The western part of the lake basin shows a similar morphology as the eastern part. However, the channels and deltaic terraces are inactive relics from periods when the Chu River, which is bypassing the lake today at its western end, was discharging into the lake. Steep slopes with sublacustrine canyons and scarps formed by mass wasting characterize the northern and southern parts of the basin.

Issyk Kul is monomictic with convective winter turnover creating a well-mixed and completely oxygenated water column (Kipfer & Peeters, 2002; Merkel & Kulenbekov, 2012). The deep-water residence time is estimated to be rather short, probably less than 15 years (Hofer et al., 2002; Kipfer & Peeters, 2002; Peeters et al., 2003). Mixing of the water column is promoted by the existence of a year-round, counter-clockwise circulation (10–12 cm s⁻¹) along the periphery of the lake accompanied by dynamic upwelling in the central part of the lake (Savvaitova & Petr, 1992; Shabunin & Shabunin, 2002; Figure 2). The circulation is caused by the Coriolis force, the lake temperature and density gradients, a southward turn of the strong and dominant western wind (“ulan”) and northward

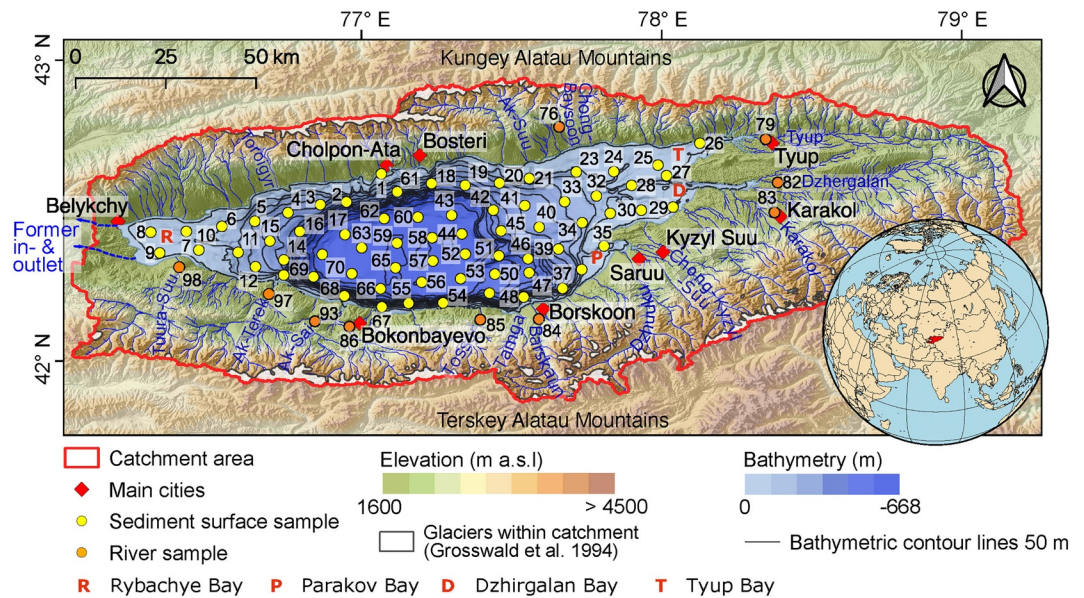


Figure 1. Topographic map of the catchment area and bathymetry of Lake Issyk Kul with the location of the study area marked on the globe. Globe was created with GMT 6.3.0 (Wessel et al., 2019).

turn of the weaker eastern (“santash”) wind after entering the basin. The lake water is slightly saline ($\sim 6 \text{ g kg}^{-1}$) (Vollmer et al., 2002) and is oversaturated with calcite, monohydrocalcite and vaterite (Giralt et al., 2002). The pH ranges from 8.75 at the lake surface to 8 at the bottom (Giralt et al., 2004), but some measurements also show a wider pH range, varying between 6.5 and 9.98 in the littoral zone and between 8.13 and 8.95 in the pelagial zone (Karmanchuk, 2002). The lake’s ion composition is characterized by Na and Mg cations as well as Cl and SO_4 anions (Karmanchuk, 2002). The thermocline shifts seasonally between 70 and 125 m water depth (Zavialov et al., 2018). Highest phytoplankton concentrations occur in water depths of $\sim 15\text{--}50 \text{ m}$ in summer, but significant algae concentrations occur down to 150 m during most of the year (Podrezov et al., 2020), which is attributed to the high water transparency (Romanovsky, 2002b). The lake is hyperoligotrophic with production rates of phytoplankton below $\sim 500 \text{ mg m}^{-3}$ and those of zooplankton below $\sim 900 \text{ mg m}^{-3}$ (Baetov, 2005). Although the area around the lake is not densely populated ($\sim 500,000$ inhabitants and similar number of tourists; Podrezov et al., 2020 and references therein), industrial activities, pollution, agriculture, and increasing water diversion for agricultural purposes cause ecological disturbances (e.g., Baetov, 2005; De Batist et al., 2002; Podrezov et al., 2020).

The regional climate is controlled by the influence of the Siberian High during winter and the Indian Low during summer (Podrezov et al., 2020; Ricketts et al., 2001). In winter, dry cold air masses lead to negligible precipitation and temperatures as low as -10°C . In summer, cyclonic occlusion generates precipitation and leads to temperatures as high as 20°C . The main moisture sources are the Mediterranean and the North Atlantic (Giralt et al., 2004; Oberhänsli & Molnar, 2012). Annual evaporation from the lake surface is about 700 mm (Giralt et al., 2004). High-altitude insolation, the slightly saline surface waters and the buffer capacity of the large lake volume with respect to temperature prevent seasonal freezing of the lake surface despite the relatively high elevation of the lake and low air temperatures during the winter months (Romanovsky, 1990). The lake functions as

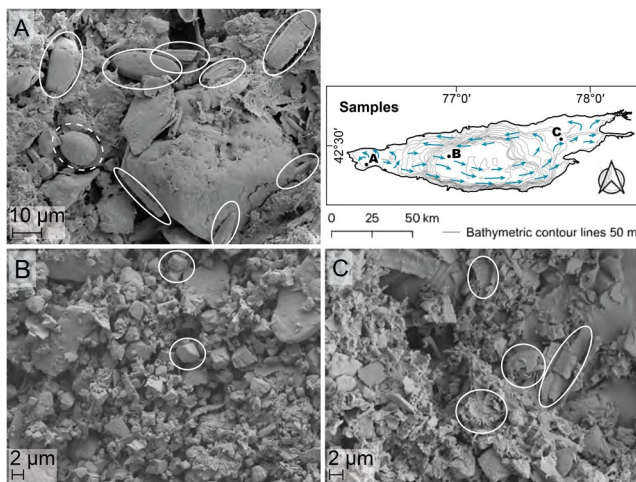


Figure 2. Scanning electron microscopy pictures from the western, central and eastern part of Issyk Kul indicating different sediment composition, such as differing contents of well-preserved (a; IK 9) to physically reworked and/or poorly preserved (c; IK 32) diatom frustules, and euhedral, rhombic carbonates with grain sizes of $2\text{--}3 \mu\text{m}$ (b; IK 17). Respective examples of well-preserved (a), physically reworked and/or poorly preserved diatoms (c), and rhombic carbonates (b) surrounded by associated sediments are indicated in the white circles. See also Figure S1 in Supporting Information S1 for light microscope images of well-preserved diatoms. The roundish body in the central left part of (a, dashed circle) most likely belongs to a testate amebae of the genus *Paulinella*. Blue arrows in the bathymetric map (top, right) depict simplified surface currents in the lake (modified from Romanovsky and Shabunin (2002)).

Table 1
The Data Set Includes 66 Sediment Surface Samples Covering the Entirety of the Lake Basin and 10 Samples From the Major Inflows

	Sample ID
Surface Sample	IK 1–21; 23–37; 39–63; 65; 67–70
River Sample	IK 76; 79; 82–86; 93; 97; 98

Note. For sample locations see Figure 1.

a heat reservoir and moisture supplier, mitigating the near shore climate. A longitudinal moisture transport caused by the strong westerly winds results in a strong gradient of rainfall. The western shore of Issyk Kul near Belykchy receives 120 mm yr⁻¹ of rainfall, whereas the eastern shore near Karakol receives 720 mm yr⁻¹ (Ricketts et al., 2001; Romanovsky, 1990). Therefore, the western plains are sparsely vegetated to barren lands, while the eastern ones are predominantly covered with grasses, shrubs and agricultural crop lands (Figure 1). A forest belt starts ~400 m above the lake and is very restricted in the western part of the lake and more extensive in its eastern part. Above, alpine and subalpine meadows and pastures dominate (Leroy et al., 2021; and references therein).

The lake is fed by 118 predominantly ephemeral inlet streams that drain the catchment area of 22,080 km² (Baetov, 2005). The inlets originate from rainfall, groundwater and meltwater from snow and high-altitude glaciers covering 3% of the catchment (Figure 1; Aizen et al., 1995; Ricketts et al., 2001). The two largest inlets (Tyup and Djyrgalan Rivers) enter the lake at its eastern shore. Smaller streams tend to seep into the coarse foreland sediments before reaching the lake and many have been diverted for irrigation, industry and urban domestic life (Merkel & Kulenbekov, 2012; Zhang et al., 2022). Issyk Kul is presently a closed-basin lake, that is, it has no surface outflow and water loss is primarily caused by evaporation (Krivoshei & Gronskaya, 1986; Romanovsky, 2002a). The lake would overflow, at the western shore, at an elevation of 1,620 m, that is, 13 m above the current lake level (Aizen et al., 1995; Ricketts et al., 2001). Here, the Kutemaldinsky threshold decoupled the Chu River from the Issyk Kul catchment at the end of the Late Pleistocene (De Batist et al., 2002 and references therein). The last activity of the outlet is reported for the 18th century (Podrezov et al., 2020; Romanovsky, 2002a).

Issyk Kul is lodged in a tectonically active compressional basin between two mountain ranges, the Terskey Alatau (max. height 5,212 m a.s.l.) to the south and Kungey Alatau (max. height 4,771 m a.s.l.) to the north (Zubovich et al., 2010). The modern orogeny results from far-field deformation of the still ongoing Indo-Asian collision that started in the Upper Eocene (e.g., Chedia, 1986; Molnar & Tapponnier, 1975; Trofimov, 1990). A progressive, southward dipping unconformity in the lake sediment infill, abundant earthquake activity, convergence rates of 5 mm yr⁻¹ between the Terskey Alatau and the Kungey Alatau, and widespread folding in the eastern, southern and north-western part of the basin bear witness of ongoing basin deformation with higher uplift rates in the south (e.g., Gebhardt et al., 2017; Zubovich et al., 2010). The bedrock geology is characterized by complex structural and lithological appearance. The lower, flat part of the catchment area is covered with Quaternary alluvial, fluvial, and glaciofluvial sediments (see e.g., Figure 2 in De Grave et al., 2013). Above, uplifted Neogene sediments are exhumed. The Kungey Alatau and Terskey Alatau are dominated by Cambrian to Silurian volcanic rocks of different origin. The eastern Terskey consists of Upper Proterozoic granitoids, Cambrian to Silurian volcanic rocks, Cambro-Ordovician gabbro, and Upper Devonian to Middle Carboniferous siliciclastic and Devonian granitoid rocks, which are all dissected by NNE-SSW faults and perpendicularly aligned SSE-NNW striking transverse thrust faults. Permian granitoids are exposed to the west of Issyk Kul (De Grave et al., 2013).

3. Materials and Methods

3.1. Sediment Sampling

During a field campaign in September 2019, surface sediment samples were retrieved from 66 sites (Table 1) along a quasi-equidistant sampling grid (average resolution of ~10 km) covering the entire lake (Figure 1). Water depths at the sampling sites range between 8 and 665 m (Figure 1). Sampling was performed using a gravity corer (UWITEC Ltd., Austria), equipped with plastic liners 60 cm long and 9 cm in diameter. The sampling device was operated with an electrical winch mounted to the research vessel “Moltur.” The supernatant water from all gravity cores was clear, indicating an undisturbed coring process. On deck, bulk samples were taken from the uppermost 2 cm of the up to ~45 cm long gravity cores. Complete gravity cores were only preserved from few sites for future analyses. According to average sedimentation rates of ~0.3 mm yr⁻¹ for deep basin sediments (De Batist et al., 2002) and somewhat higher rates of up to 1 mm yr⁻¹ for sediments deposited on the western and eastern platforms (e.g., Giralt et al., 2002; Leroy et al., 2021; Rasmussen et al., 2000; Ricketts et al., 2001), the uppermost 2 cm of surface sediment samples should integrate over ca. 30–100 years. Another set of 10 sediment

Table 2

The Multiproxy Approach Included Energy Dispersive X-Ray Fluorescence (EDXRF) Analysis, Measurement of Total Inorganic and Organic Carbon (TIC, TOC), Nitrogen (TN), and Grain-Size Distribution, Analyses of *n*-Alkanes, Alkenones, Glycerol Dialkyl Glycerol Tetraether (GDGTs), and Diatoms as Well as Scanning Electron Microscope (SEM) Images

Method	EDXRF	TN	TIC, TOC	Grain size	<i>n</i> -Alkanes, Alkenones	GDGTs	Diatoms	SEM
Sample ID	IK 1–21; 23–37; 39–63; 65; 67–70; 76; 79; 82–86; 93; 97; 98	IK 1–21; 23–37; 39–63; 65; 67–70;	IK 1–21; 23–37; 39–63; 65; 67–70; 76; 79; 82–86; 93; 97; 98	IK 1–21; 23–37; 39–63; 65; 67–70;	IK 1; 8; 10; 11; 15–17; 19; 25; 26; 28; 32; 33; 41–43; 45; 47–49; 51; 55–58; 60–62	IK 10; 11; 15–17; 19; 25; 28; 32; 33; 41–43; 45; 47–49; 51; 60; 62	IK 1–11; 15–17; 19; 21; 24–26; 28; 30–35; 39; 41–43; 47; 49; 51; 55–60; 62; 63; 69; 70	IK 9; 15; 17; 25; 28; 32; 33; 42; 60

Note. The different analyses were done at different sample resolution.

samples (Table 1) was taken from the major inlets (Figure 1). All samples were stored in plastic bags and shipped to the University of Cologne, Germany, for further analyses.

3.2. Analytical Work

At the University of Cologne, all samples were freeze dried. Smear slides were sporadically taken for the identification of sedimentary components using transmitted light microscopy. Scanning electron microscope (SEM) images on samples IK 9, 17, and 32 (Figures 1 and 2) were produced with a Sigma 300 VP (Zeiss, Germany) after sputtering with Au.

Element concentration analyses on both the sediment surface and river samples ($n = 76$; see Table 2) was conducted by energy dispersive X-ray fluorescence spectrometry (EDXRF). Before measurement, 5 g of each sample was homogenized, milled $<63 \mu\text{m}$ and pressed into 32 mm pellets after adding 1 g of Cereox binder licowax (Fluxana GmbH & Co KG, Germany). Measurements were carried out using a SPECTRO XEPOS He (SPECTRO Analytical Instruments Ltd., Germany) analyzer in a helium gas atmosphere. The contents of all elements from sodium to uranium were simultaneously determined and adjusted to sample weight. Measurements were performed in duplicate. Average values of two measurements were calculated (standard deviation $<5\%$) for each sample and used for interpretation.

Analyses of total carbon (TC), total inorganic carbon (TIC), total nitrogen (TN), and grain-size distribution were performed on 66 sediment surface samples (Table 2). For TC, TIC and TN measurements, sample aliquots of approximately 100 mg were homogenized and milled $<63 \mu\text{m}$. TN concentrations were measured using a Vario MICRO Cube elemental analyzer (Elementar Corp., Germany) after combusting the material in small tin capsules at $1,150^\circ\text{C}$. A DIMATOC 2000 carbon analyzer (Dimatec Corp., Germany) was used to measure TC after combusting the material at 900°C and TIC after treatment with phosphoric acid (H_3PO_4) and combustion at 160°C . Total organic carbon (TOC) was calculated from the difference between TC and TIC. The TOC/TN ratio was determined from the TOC and TN contents using a factor of 1.167 to obtain the atomic ratio (Meyers & Terranes, 2001). The minerogenic origin of TIC was checked in selected samples by means of SEM imagery. The calcite content (CaCO_3) was calculated by multiplying TIC with the stoichiometric factor of 8.33.

For grain-size analyses, approximately 1 g of each surface sediment sample ($n = 66$; Table 2) was treated with 35% hydrogen peroxide (H_2O_2), 10% hydrochloric acid (HCl), 1 M sodium hydroxide (NaOH), and sodium hexametaphosphate ($\text{Na}_6\text{O}_{18}\text{P}_6$) for removal of organic matter (OM), carbonate, biogenic silica, and sample dispersion, respectively (Francke et al., 2013). Each step was repeated until notable reactions completely ceased. In between these steps, the samples were washed with ultrapure water until pH neutralization. Grain-size analyses were carried out using a Beckman Coulter LS13 320 Laser Diffraction Particle Size Analyzer (Beckman Coulter, USA). Results were calculated by averaging three measurements of each sample and are given in volume percentages (vol %) for grain-size classes between 0.04 and $2,000 \mu\text{m}$. The gravel-bearing samples 27 and 29 were sieved with mesh sizes between 63 and $2,000 \mu\text{m}$.

For lipid biomarker analyses, 28 surface sediment samples forming one west-east and two north-south transects across the lake have been processed. About 1–10 g sediment was ultrasonically extracted using a mixture of dichloromethane (DCM) and methanol (MeOH) (2:1; v:v), repeated 3 times. The extracts were combined and the bulk of the solvent was removed by rotary evaporation under vacuum. Subsequently, the total lipid extracts were separated into apolar (*n*-alkanes), ketone (alkenones), and polar (Glycerol Dialkyl Glycerol Tetraether, GDGTs) fractions by column chromatography using activated silica gel and eluting with *n*-hexane, DCM, and DCM:MeOH (1:1, v:v), respectively. The apolar and ketone fractions were dissolved in *n*-hexane prior to analysis. The polar fractions were dissolved in *n*-hexane:isopropanol (95:5; v:v) and filtered through $45 \mu\text{m}$ PTFE syringe filters previous to analysis. Internal and external standards (C_{46} -GDGT, 2-nonadecanone, *n*-alkane (C_{21} - C_{40}) standard solution) were used for quantification and compound identification.

Analyses of *n*-alkanes and alkenones ($n = 28$; Table 2) were carried out with a gas chromatograph fitted with an on-column injector and flame ionization detector (GC-FID; HP 5890). A fused silica capillary column (Agilent DB-5MS; $50 \text{ m} \times 0.2 \text{ mm}$, film thickness: $0.33 \mu\text{m}$) was used with He as carrier gas. Samples were injected at 70°C and the GC oven temperature was subsequently raised to 150°C at a rate of $20^\circ\text{C min}^{-1}$, and then at 6°C min^{-1} to 320°C (that was held 40 min). The analytical precision based on replicate measurements of our in-house sediment standard was in general $<0.2^\circ\text{C}$.

GDGT analyses were conducted on 20 out of the 28 processed samples (Table 2). Measurements were performed according to Hopmans et al. (2016) using ultrahigh performance liquid chromatography (UHPLC; Agilent 1290 Infinity) coupled to a 6460 Triple Quad—atmospheric pressure chemical ionization—mass spectrometer (TQ-APCI-MS; Agilent Technologies, USA). To improve separation, two UHPLC silica columns (BEH HILIC columns, 2.1, 150 mm, 1.7 μm ; Waters) were coupled in series and fitted with a 2.1-cm-long, 5-mm-diameter pre-column of the same material. Individual GDGTs were detected via single ion monitoring (SIM).

For data evaluation, the programs OpenLab CDS and Mass Hunter Qualitative Analyses from Agilent Technologies were used.

n-Alkane chain-length distributions were used to distinguish between sources from aquatic algae and phytoplankton (C_{17} and C_{19}), moss and aquatic macrophytes (C_{21} , C_{23} , C_{25}), trees and shrubs (C_{27} and C_{29}), and grasses (C_{31} and C_{33}) (Ficken et al., 2000; Meyers & Ishiwatari, 1993). The average chain length (ACL) describes the relative distribution of odd-carbon-numbered higher plant *n*-alkanes (C_{27} – C_{33}) (Eglinton & Eglinton, 2008) to distinguish between different vegetation types (Ficken et al., 2000; Meyers & Ishiwatari, 1993):

$$\text{ACL}_{27-33} = (27 * C_{27} + 29 * C_{29} + 31 * C_{31} + 33 * C_{33}) / (C_{27} + C_{29} + C_{31} + C_{33})$$

The carbon preference index (CPI), captures the odd over even chain-length distribution of *n*-alkanes (Bray & Evans, 1961):

$$\text{CPI}_{27-33} = 1/2 * [(C_{27} + C_{29} + C_{31} + C_{33}) / (C_{26} + C_{28} + C_{30} + C_{32}) + (C_{27} + C_{29} + C_{31} + C_{33}) / (C_{28} + C_{30} + C_{32} + C_{34})]$$

Both ACL and CPI can be used to characterize the quality of organic matter, with lower values pointing to enhanced degradation or input of petrogenic sources.

The alkenone unsaturation index, $U_{37}^{k'}$, is based on the relative proportions of disaturated and triunsaturated alkenones produced by haptophyte algae (Prahl & Wakeham, 1987):

$$U_{37}^{k'} = C_{37:2} / (C_{37:2} + C_{37:3})$$

Prahl et al. (1988) proposed an empirical relationship between the $U_{37}^{k'}$ -index and growth temperature (T) based on cultured *Emiliania huxleyi*:

$$U_{37}^{k'} = 0.034 * T + 0.039 \quad (R^2 = 0.99)$$

Müller et al. (1998) revised this calibration based on extensive alkenone analyses on a global set of marine core-top samples:

$$U_{37}^{k'} = 0.033 * T + 0.044 \quad (R^2 = 0.96; \text{RMSE} = 1.5^\circ\text{C})$$

The distribution of branched GDGT (brGDGT), presumably membrane lipids of soil bacteria, can be used to calculate mean annual air temperature (MAT) based on the degree of methylation and cyclization of brGDGTs (MBT and CBT) (Peterse et al., 2012):

$$\text{MBT}' = (\text{Ia} + \text{Ib} + \text{Ic}) / (\text{Ia} + \text{Ib} + \text{Ic} + \text{IIa} + \text{IIb} + \text{IIc} + \text{IIIa})$$

$$\text{CBT} = -\log((\text{Ib} + \text{IIb}) / (\text{Ia} + \text{IIa}))$$

$$\text{MAT} = 0.81 - 5.67 * \text{CBT} + 31.0 * \text{MBT}'$$

The global soil calibration of De Jonge et al. (2014) allows temperature reconstruction independent of pH:

$$\text{MAT}_{\text{mr}} (\text{°C}) = 7.17 + 17.1 * [\text{Ia}] + 25.9 * [\text{Ib}] + 34.4 * [\text{Ic}] - 28.6 * [\text{IIa}]$$

$$(R^2 = 0.68; \text{RMSE} = 4.6^\circ\text{C})$$

Roman numerals refer to fractional abundances of bacterial branched GDGTs (brGDGTs) in soils (see De Jonge et al., 2014 for GDGT chemical structures). RMSE is the root-mean-squared error of temperature in the respective calibration.

More recently, Raberg et al. (2021) proposed two new calibrations for general use in lake sediments, which were specifically recommended for areas characterized by low MAT and high seasonality, and therefore most likely experience a warm-season bias. As Issyk Kul is exposed to high seasonality, we additionally calculated the mean temperature of months above freezing (MAF) using compound fractional abundances within a structural set of brGDGTs:

$$\begin{aligned} \text{MAF } (^{\circ}\text{C}) = & 92.9 + 63.84 \times \text{fIb}_{\text{Meth}}^2 - 130.51 \times \text{fIb}_{\text{Meth}} - 28.77 \times \text{fIIa}_{\text{Meth}}^2 - 72.28 \times \text{fIIb}_{\text{Meth}}^2 - 5.88 \times \text{fIIc}_{\text{Meth}}^2 \\ & + 20.89 \times \text{fIIIa}_{\text{Meth}}^2 - 40.54 \times \text{fIIIa}_{\text{Meth}} - 80.47 \times \text{fIIIb}_{\text{Meth}} \\ & (R^2 = 0.90; \text{RMSE} = 2.1^{\circ}\text{C}) \end{aligned}$$

Diatom analyses were conducted on 44 samples (Table 2) across the lake. Techniques in Battarbee et al. (2001) were adopted for diatom slide preparation, with ~0.1 g freeze-dried sediment samples treated with 30% H₂O₂ to oxidize OM and a few drops of concentrated HCl to remove carbonates. Known quantities of microspheres were added to allow the calculation of absolute valve concentration. Slides were mounted using Naphrax™. Diatoms were counted at 1,000× magnification under oil immersion on a Leica DM2500 light microscope. More than 300 valves per sample were counted, and diatom fragments were also counted for the assessment of diatom preservation using the *F*-index, that is, the ratio of pristine valves to total valves (Ryves et al., 2001). Diatom identification was based on a range of classic literature (Krammer & Lange-Bertalot, 1986, 1988, 1991a, 1991b).

3.3. Statistical Data Analyses and Graphic Display

Statistical data-processing of grain-size raw data was carried out with the GRADISTAT software (Blott & Pye, 2001). The processed grain-size data were converted to three end members (EM) using the MatLab-based AnalySize software (Paterson & Heslop, 2015; The MathWorks Inc, 2021).

Spatial interpolation of the surface sediment data using the kriging method and the subsequent graphic display of the results was accomplished with Surfer® version 9.11 (Golden Software, LLC) and QGis-3.4.10 Madeira (Team, 2022).

Multivariate principal component analysis (PCA) was applied to selected quantitative EDXRF (Fe, Ti, Zr, Al, Rb, Si, K, Mn, Ca) and biochemical (TOC, TN) variables to explore the grouping of subsamples according to their similarities (e.g., Bro & Smilde, 2014). PCA was performed using the Palaeontological Statistics software (PAST4 v. 4.11; Hammer et al., 2001) applying a correlation matrix. End members (EM1, EM2, EM3), water depth, longitude and latitude (transferred to UTM metric scale), and TOC/TN ratio of surface sediment locations and samples were added as supplementary variables to identify the generic origin of the sedimentary components and the process systems of sediment deposition.

4. Results

The surface samples of Issyk Kul mostly consist of silt with varying amounts of finely dispersed OM, plant remains, calcareous macrofossils (e.g., gastropods), microfossils (diatom frustules) and carbonate minerals. The SEM photos of surface sediment samples of the lake illustrate distinct variations in composition. Note here, for example, the differing contents of well-preserved diatom frustules in the western part (Figure 2a) to physically reworked and/or poorly preserved frustules in the eastern part (Figure 2c), and euhedral, rhombic carbonates with grain sizes of 2–3 μm in the central part (Figure 2b).

4.1. Quantitative EDXRF Element Data of the Surface Sediment Samples

Concentrations of Al (3.3–8.5%), Fe (2.0–4.2%), K (1.0–3.0%), Ti (0.2–0.5%), Rb (0.01–0.02%), Si (8.6–27.3%), and Zr (0.01–0.02%) are highest in the surface sediment samples along the lake's southern and eastern periphery, especially where the major rivers enter the lake (samples IK 13, 14, 26, 35, 48, 49, 54, 67, 68; Figure 3). Exception are samples from the Dzhergalan Bay, where rivers Dzhergalan, Karakol, and Irdyk enter the lake and where only Al, K, Rb and Si are high (samples IK 27, 29, 30). Here, the sum of the individual concentrations of the elements Al, Fe, K, Ti, Rb, Si, and Zr, hereafter referred to as SUM clastic, is nevertheless highest (Figure 3). The surface sediments from the steep southern slope show elevated values of SUM clastic down to ~550 m water depth (samples IK 49, 69), while they are restricted in the Tyup, Dzhergalan, and Parakov Bays to the upper 80 m.

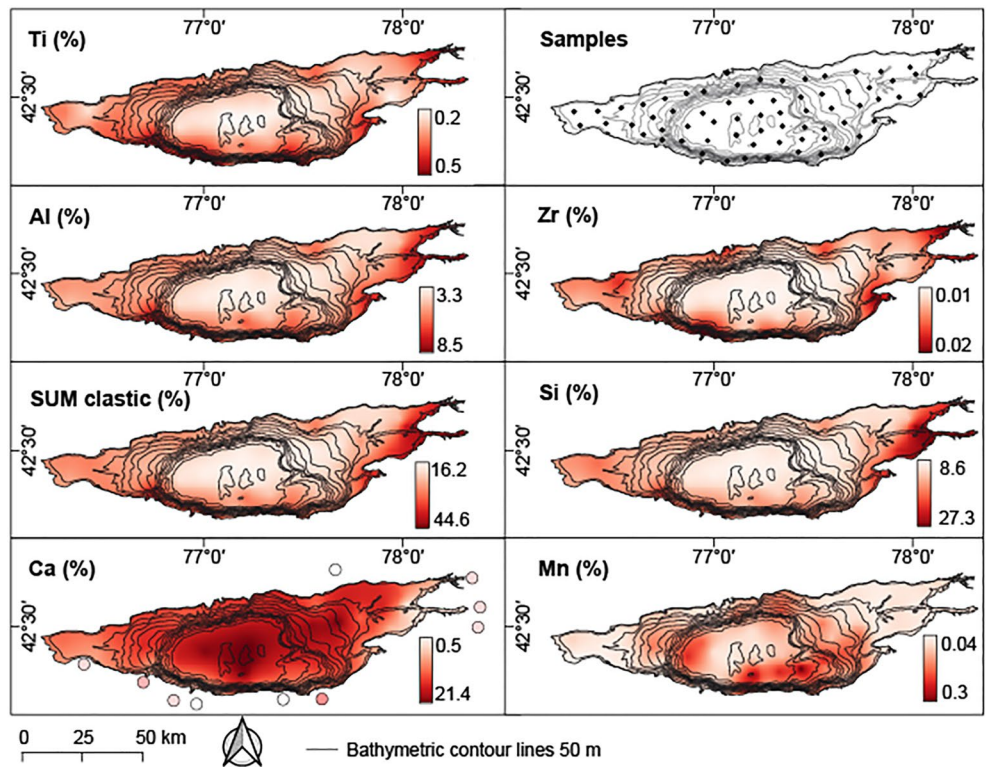


Figure 3. Selected quantitative EDXRF element data of surface sediment samples. Spatial interpolation is based on 66 data points (Table 2) marked as black dots (upper right box). Ca was also measured at 10 inlet samples (colored according to scale; see also Figure 1 for locations). The relative abundance pattern for Ti is similar to Fe, but Fe has different concentrations. The relative abundance pattern for Al is similar to K and Rb, but K and Rb have different concentrations.

Besides the spotty maxima in front of the southern (and eastern) tributaries, Al, Fe, K, Ti, Rb, Si, and Zr are also slightly elevated in front of the northern river mouths to water depths <80 m (samples IK 1, 21). Furthermore, Al, Fe, K, Ti, Rb, Si, and Zr concentrations are slightly elevated throughout the western shelf area to water depths of ~300 m (samples IK 2–12, 15, 16).

Concentrations of Ca (0.5–21.4%) are, in contrast to the spatial distribution of the elements Al, Fe, K, Ti, Rb, Si, and Zr, relatively low in front of major river mouths at the southern (0–550 m), eastern (<80 m), and northern shore (around sample IK 21; <80 m), especially in the Dzhergalan Bay (samples IK 27, 29, 30; Figure 3). Throughout the western shelf area in water depths <100 m (samples IK 6–11), Ca concentrations are around 10%. Below these depths, Ca concentrations increase toward the lake center, with highest concentrations of ~20% at water depths >600 m (samples IK 56–59, 63, 65).

Mn (0.04–0.3%) is locally elevated, especially around samples IK 70, 56, 53, and 50 (Figure 3), where Mn maxima are edging the slope foot of the deep central basin.

4.2. Total (in)organic Carbon and Nitrogen Data of the Surface Sediment Samples

TIC contents vary between 0.4% and 7.3% and show the same spatial distribution as Ca concentrations (Figures 3 and 4). Shell fragments from gastropods and molluscs, particularly in samples from shallower sites, as well as ostracods that have been used for radiocarbon dating and stable isotope studies of sediment cores (e.g., Leroy et al., 2021) likely contribute to the TIC contents. However, the SEM results (Figure 2) demonstrate that inorganic

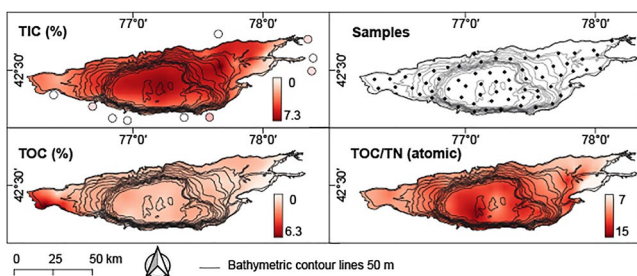


Figure 4. Total inorganic carbon (TIC), total organic carbon (TOC), and total nitrogen (TN) data of surface sediment samples from Issyk Kul. Spatial interpolation includes 66 surface sediment samples (Table 2) marked as black dots (upper right box). The relative abundance pattern for TN is similar to TOC, but TN has different concentrations. TIC was also measured at 10 inlet samples (colored according to scale; see also Figure 1 for locations).

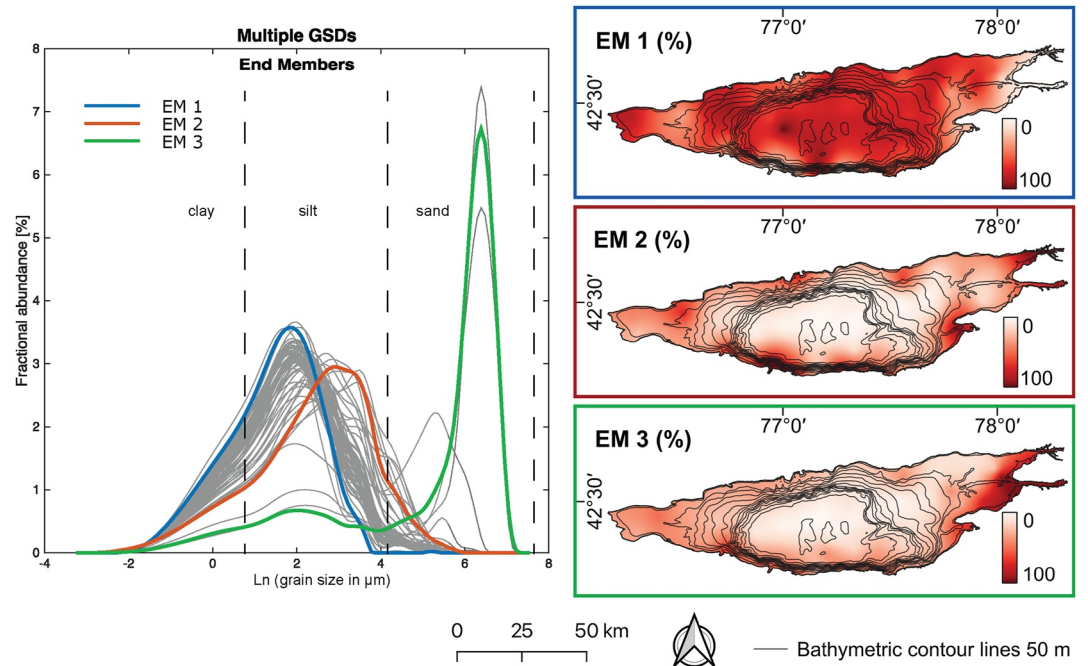


Figure 5. Multiple grain-size distributions (GSDs) of the Issyk Kul surface sediment samples together with three associated End Members (EM1–3). Dashed lines indicate boundaries of clay, silt, and sand. The multiple specimen plot (left side) does not include the very coarse-grained samples IK 27 and 29, because they plot outside the displayed data limits. Sample sites are the same as shown in Figure 3.

carbon is predominantly represented by idiomorphic, rhombic carbonates with grain sizes of 2–3 μm . In areas <100 m water depth TIC contents are on average 3%, which corresponds to a CaCO_3 content of $\sim 25\%$. In the deep, central basin TIC contents average at 6%, which indicates that CaCO_3 forms up to 60% of these sediments.

The TOC and TN contents range from 0.1% to 6.4% and 0–0.8%, respectively (Figure 4). They show a similar spatial distribution with maxima in the south-western Rybachye Bay (<50 m) and lower values in front of major rivers, especially in the vicinity of the Dzhergalan Bay (<50 m). TN contents show a slight decrease toward the deep, central part of the lake basin.

The $\text{TOC}/\text{TN}_{\text{atomic}}$ ratios range between 7 and 15, except from samples 29 and 30, which have $\text{TOC}/\text{TN}_{\text{atomic}}$ ratios of 29 and 105, respectively (Figure 4). Slightly higher $\text{TOC}/\text{TN}_{\text{atomic}}$ ratios apparently occur with increasing water depths. In water depths <100 m the $\text{TOC}/\text{TN}_{\text{atomic}}$ ratios are around 10, whereas in the deep, central basin, ratios are around 12.

4.3. Quantitative Ca and Total Inorganic Carbon Data of the River Samples

Ca concentrations and TIC contents are relatively low in the river samples (averaging at 4.0% TIC) compared to the sediment surface samples (averaging at 0.7% TIC; Figures 3 and 4). Highest Ca concentrations and TIC contents in the river inlets are recorded in the south-eastern part of the catchment (IK 84), with 8.91% and 2.15%, respectively. The large difference to the western, neighboring site (IK 85), which is 15 km apart and has Ca and TIC of 1.41% and 0.05%, respectively, shows a large local impact of the bedrock geology in the catchment and/or biases from grain-size effects in the individual samples.

4.4. Grain-Size Data

The grain-size distribution of surface sediments throughout the lake (Figure 5) is highly variable, although most of the sediments show silt contents between 72.4% and 82.1%. The grain-size distribution is reflected by 3 nonparametric EMs, which explain 96.8% of the data set variance and 99.4% of the median variance of the samples (Figure 5). EM1 includes an average of 46.0% clay, 53.9% silt, and 0.1% sand, EM2 25.7% clay, 72.9%

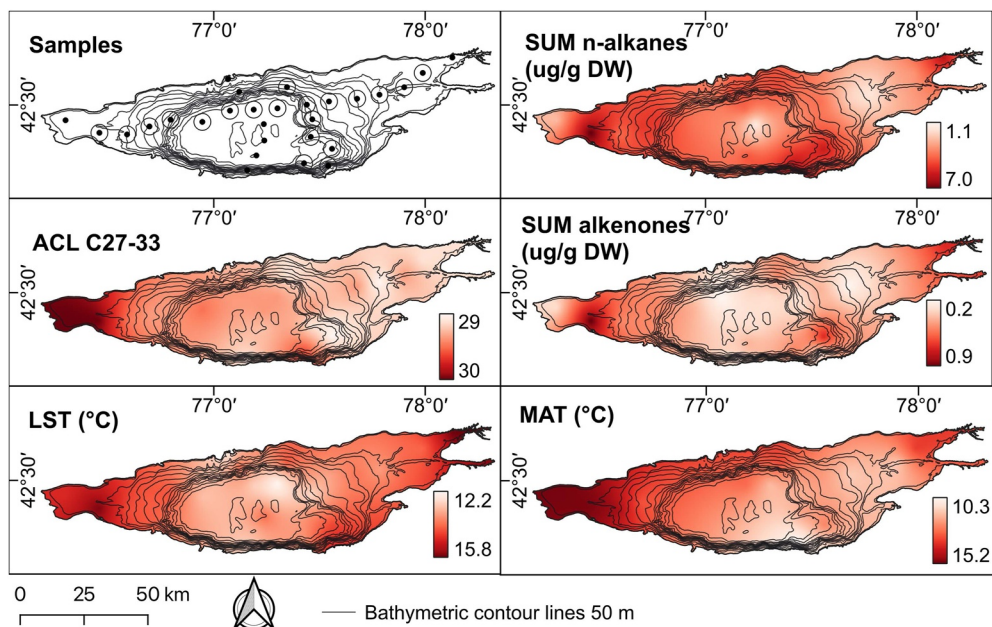


Figure 6. Selected biomarker data. Samples for *n*-alkanes and alkenones analyses ($n = 28$) are displayed as black dots, while those for Glycerol Dialkyl Glycerol Tetraether (GDGT) analyses ($n = 20$) are marked with unfilled circles in the upper left box. For better illustration lake surface temperatures (LST) and Mean annual Air Temperature (MAT) are visualized without IK 58.

silt, and 1.4% sand and EM3 0.2% clay, 0.3% silt, and 99.5% sand. The spatial distribution clearly indicates that EM1 dominates in the deep basin and represents the hemipelagic, undisturbed sedimentation in the lake basin where very low transport energies prevail (Savvaitova & Petr, 1992). In contrast, EM2 and 3 show generally high values in the shallower lake areas and close to the shoreline, in particular in the vicinity of major river inlets, that rapidly decrease toward more distal locations and the center of the lake. In the Dzhergalan Bay, at water depths above 18 m, EM3 is up to 73.3%.

4.5. Biomarker Data

Concentrations of *n*-alkanes (SUM *n*-alkanes) are between 1.1 and 7.1 $\mu\text{g g}^{-1}$ dry weight (DW) (Figure 6). Concentrations are generally high around the northern, southern and western (except IK 8) shore of Issyk Kul and decrease toward the lake center (except IK 56). Lower concentrations occur also in the eastern upper and lower shelf areas or platforms, respectively (except in Tyup Bay, IK 26). Highest proportion of *n*-alkanes are derived from land plants (C_{27} , C_{29} , C_{31} , and C_{33} ; 0.6–3.7 $\mu\text{g g}^{-1}$ DW). Lower proportions originate from aquatic macrophytes (C_{21} , C_{23} , C_{25} ; 0.2–1.5 $\mu\text{g g}^{-1}$ DW) and from algal primary production (C_{17} and C_{19} ; 0.0–0.7 $\mu\text{g g}^{-1}$ DW). The ACL shows a slight longitudinal trend and decreases from around 30 in the western part of Issyk Kul to around 29 in the east (Figure 6). CPI is >8.2 in all surface sediments.

Concentrations of alkenones (SUM alkenones) range from 0.2 to 0.9 $\mu\text{g g}^{-1}$ DW with partially higher values in shallow areas and along the slopes and low values in the deep basin (>550 m; Figure 6). Lake surface temperatures (LSTs) calculated in accordance with Prah et al. (1988) range from 12.0 to 15.4°C (average of 13.3°C), while LSTs estimated after Müller et al. (1998) vary from 12.2 to 15.7°C (average of 13.6°C; Figure 7), except from IK 58, where LSTs are 7.6 and 7.7°C, respectively. LSTs (Müller et al., 1998; Prah et al., 1988) display quite similar spatial distribution patterns with higher temperatures in the western and eastern shallow lakes areas (especially IK 8, 10, and 26) and colder temperatures basinward and close to sites IK 1 and 55, located in proximity to the northern and southern shores.

MAT estimates (Peterse et al., 2012) are between 5.7 and 10.5°C (average of 8.3°C). Higher MAT estimates of 10.3–15.0°C (average of 12.4°C) result from the calibration of De Jonge et al. (2014). Both calibrations show highest values in the uppermost ~ 100 m of the western lake basin (Figure 7). MATs are higher along the northern

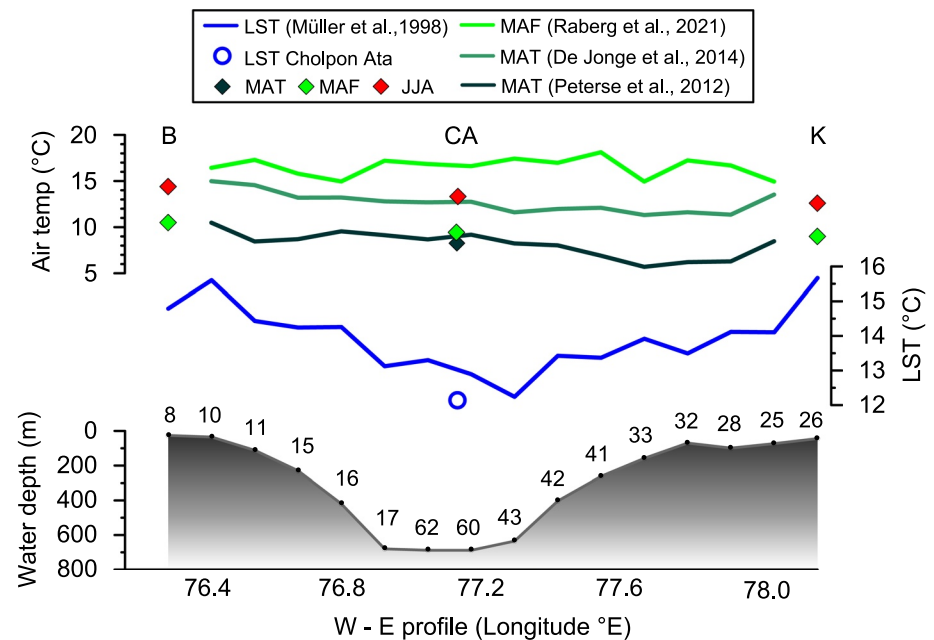


Figure 7. West-east profile with alkenone-inferred temperature reconstructions for lake surface temperatures (LST; blue line according to Müller et al., 1998) and measured LST (blue circle) at Cholpon Ata (CA) for the period 1972–2009 (Romanovsky et al., 2013). Mean annual air temperatures (MAT; black line according to Peterse et al., 2012 and dark green line according to De Jonge et al., 2014) and measured MAT (black diamond) from Cholpon Ata for the period 1972–2009 (Romanovsky et al., 2013). Mean temperature of months above freezing (MAF; light green line according to Raberg et al., 2021) and measured MAF (green diamonds) from cities Belykchy (B, left) and Karakol (K, right) from the period 1991–2021 (www.climate-data.org). Also displayed are summer temperatures (June, July, and August (JJA, red diamonds) from cities Belykchy (B, left), Cholpon Ata (CA, central), and Karakol (K, right) from the period 1991–2021 (www.climate-data.org). IK 58 is not displayed, as it is obviously an outlier.

as compared to the southern slope and particularly low in the south-eastern part of the lake. In contrast, MAF estimates (Raberg et al., 2021) range between 12.2 and 18.1°C (average of 16.2°C) and reveal a slightly different pattern along the W-E profile (Figure 7).

4.6. Diatom Data

Diatoms in Issyk Kul include benthic (mostly *Amphora pediculus*, Kützing, Grunow), planktonic (mostly *Pantocselciella minuscula*, Jurilj, Williams & Round) and facultative planktonic (mostly *Pseudostaurosira brevistriata*, Grunow, Williams & Round and *Staurosirella pinnata*, Ehrenberg, Williams & Round) species (selected species shown in Figure S1 in Supporting Information S1). Diatom valve concentrations vary between 1×10^6 and 469×10^6 valves g^{-1} DW with the highest values in samples from <50 m water depths, particularly in the western part of the lake (samples IK 8, 10; Figure 8). Benthic diatom concentrations (average of 51%, up to 97%) are highest in the lake's eastern and northern part, in particular where water depths do not exceed 100 m. In the western part (Rybachye Bay; ≤ 50 m) and in the south-east of the lake, in front of the city Borskoon (sample IK 37), the highest facultative planktonic diatom concentrations (average of 22%, up to 97%) can be observed. As facultative planktonic diatoms are originally benthic but also survive when suspended in the water column, their distribution is nearly opposite to that of planktonic diatoms. The highest planktonic diatom concentrations (average of 27%, up to 72%) occur in the central deep basin (>600 m), the southern slope (entire water column) and on the eastern deep shelf area at >100 m water depths. Diatom preservation is high (*F*-index average of 93%; Figure S2 in Supporting Information S1) and its assemblage composition is dominated by small species. The *F*-index furthermore indicates that diatoms from the samples of water depths <200 m are overall better preserved than those from greater water depths (Figure S2 in Supporting Information S1).

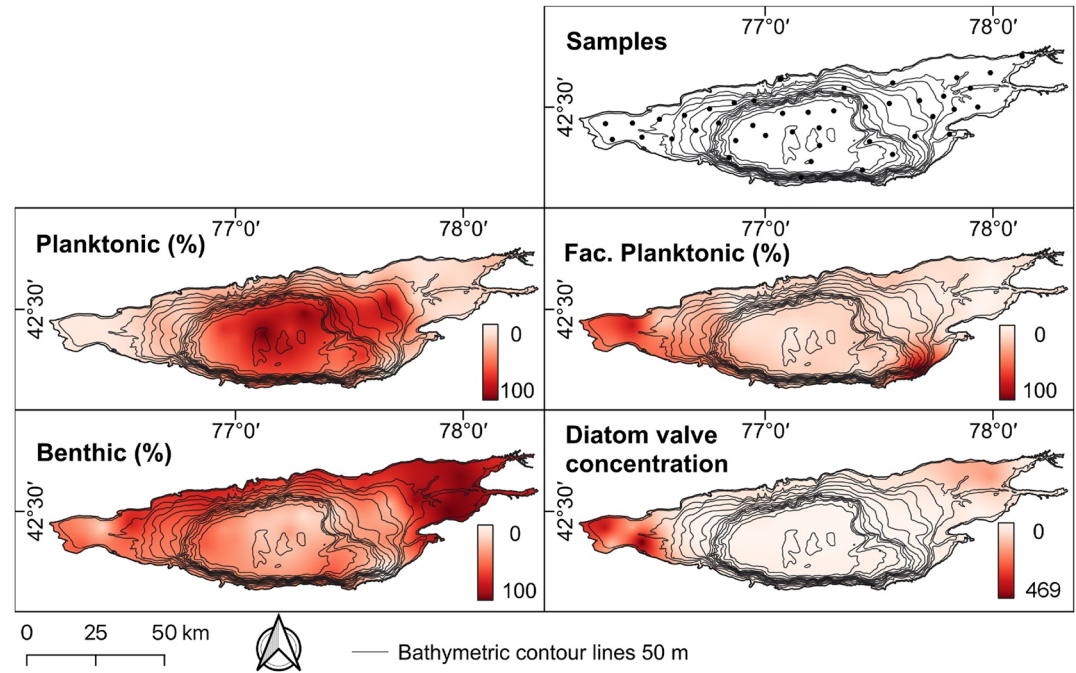


Figure 8. Selected diatom data and diatom valve concentrations ($\times 10^6$ diatoms g^{-1}). Diatom taxa include planktonic, facultative planktonic and benthic species. Spatial interpolation is based on 44 surface sediment samples marked as black dots in the upper right box.

4.7. PCA

Principal components 1 and 2 explain 57% and 22% of the data variance, respectively (Figure 9a). Component 1 shows a positive loading of Al, Fe, K, Ti, Rb, Si, and Zr, which corresponds to the supplementary variable EM2. Out of these variables, two clusters (Fe, Ti, Zr, and Al, Si, Rb, K) may be tentatively distinguished. The negative loading of component 1 is primarily driven by the elements Ca, TIC, and Mn and corresponds with supplementary variables EM1, longitude (easting), water depth, and TOC/TN. Principal component 2 demonstrates a

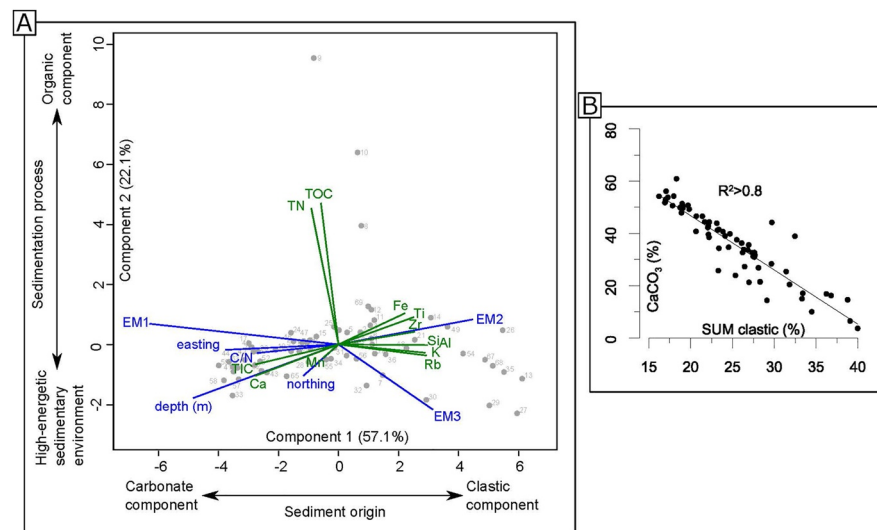


Figure 9. (a) Principal Component analyses (PCA) based on selected (bio)chemical variables (green) of surface sediment samples with the associated scatter plot and supplementary variables (EMs, northing (latitude), easting (longitude), water depth, TOC/TN ratio), which are not included in the ordination (blue). The results show groupings of the different variables according to their similarities. (b) Cross-plot of the two major components carbonate ($CaCO_3$) and detritus (SUM clastic).

positive loading of TOC and TN (organic matter) and weak negative loading of latitude and EM3. The biplot of the summed total concentrations of Al, Fe, K, Ti, Rb, Si, Zr versus the concentration of CaCO₃ shows a negative correlation with $R^2 > 0.8$ (Figure 9b).

5. Discussion and Interpretation

5.1. Clastic Input

Highest quantities of siliciclastic input (SUM clastic) are recorded in the Dzhergalan Bay and indicate that the main source of terrigenous sediment supply is associated with the rivers Dzhergalan, Karakol, and Irdyk. The Dzhergalan Bay is further characterized by highest proportions of EM3, which implies that the highest quantities of clastics are deposited in a relatively high-energetic sedimentary environment coincident with the region with the most rainfall (Ricketts et al., 2001; Romanovsky, 1990). The result corresponds with highest river inflow and sediment input from the Dzhergalan River (De Batist et al., 2002), as well as from the second largest river Tyup. Relatively high transport energies in the Dzhergalan Bay extending several kilometers basinward (samples IK 26, 27, 29, 30), are in accordance with recent hydrological measurements, which indicate that >50% of total surface discharge into the lake are provided by rivers Dzhergalan, Karakol, and Dzhuuuku, which receive considerable runoff from snow and glacial meltwater from the highest parts of the Terskey Alatau Mountains (Alifujiang et al., 2021). However, relatively low EM3 and EM2 proportions on the lower platform or in the interlobe channels (e.g., sample IK 28) indicate that the influence of the river inlets decreases toward the basin center rapidly today. This could have been different in former times, for example, during the Late Pleistocene to mid Holocene, when lake level was lower and nowadays submerged channels deeply incised into the lower platform of the eastern shelf area, forming proximal and distal delta deposits (De Batist et al., 2002). Southern and northern tributaries predominantly deposit siliciclastic sediments of EM2, which indicates that the influence of these inlets is much lower compared to the water and sediment input from the eastern rivers. However, the supply of siliciclastic sediments is higher (SUM clastic) in the south, which may to some extent be explained by higher uplift and, hence, erosion rates here (Zubovich et al., 2010). Another explanation comprises significant differences in the glaciation extent of the surrounding mountain ranges (Dikich, 2004). Whereas about 80% of the glaciers are located in the Terskey Alatau Range to the south, only 20% occupy the Kungey Alatau Range to the north (Dikich, 2004; Savvaitova & Petr, 1992; Sevastyanov & Smirnova, 1986). The Kungey Alatau Mountains, therefore, only contribute a small percentage of the total discharge into Issyk Kul (Alifujiang et al., 2021). Moreover, the southern tributaries of Issyk Kul transport the sediment much further basinward and into much greater depths (up to 550 m), as compared to the northern tributaries, where the shelf area is wider and the subaquatic slopes are less steep.

In the western extremity of the lake, relatively low river discharge (Savvaitova & Petr, 1992) may explain the siliciclastic input with dominance of hemipelagic sediments of EM1. In the deep, central basin only small quantities (SUM clastic) of siliciclastic material, likely consisting of the suspended load from rivers and distal turbidite facies, accumulate. The uniform distribution of hemipelagic sedimentation (EM1) across the deep basin argues for only weak bottom-water current activity. Stronger bottom-water currents would likely cause irregularities in sediment composition throughout the central basin depression, particularly around distinct morphological barriers, such as the anticlinal ridge in the eastern part of the central basin (see Figure 1; Ceramicola et al., 2001; De Batist et al., 2002).

As the SUM clastic shows a very similar spatial distribution to Si (Figure 3) silicon may primarily originate from weathering of siliciclastic rocks in the catchment (Savvaitova & Petr, 1992). Particularly in the western, shallow part of the lake, the correlation of Si with the diatom valve concentration indicates that Si is also derived from primary productivity, for example, diatoms, which are abundant in the SEM images from this part of the lake (Figures 2 and 8).

5.2. Redeposition of Sediments

Although the dominance of EM2 and EM3 in water depths of <100 m is partly controlled by inlets, it is supported by wave action, which may lead to resuspension and redeposition of sediments, for example, the transport of fine-grained material into deeper parts of the lake, which are less affected by wave action. Waves of up to 4 m height were reported during storm events (Podrezov et al., 2020). Such wave heights would correspond to up

100 m long waves and may affect sediment redeposition up to several tens of meters depth (e.g., Håkanson, 1977; Johnson, 1980). A good measure for a decreasing influence of wave action with increasing water depth is the existence of a shell zone, where dead shells and shells fragments accumulate. For example, at Lake Ohrid in North Macedonia, such a shell zone is reported at 20–35 m water depth (Albrecht & Wilke, 2008). Issyk Kul is much larger and oriented along the main wind axis from west to east, so it is very likely that this horizon is much deeper in Issyk Kul, likely extending to >50 m water depth. In these shallower parts, resuspension of fine-grained material during storms and periods with increased wave activity is likely to occur and may lead, in combination with supply of coarse-grained material from the inlets, to a higher proportion of coarse sediments.

Remobilization of shallow-water sediments along the steep slopes into the deep basin of Issyk Kul as a result of gravitational slope failure can be triggered by for example, earthquakes (Gebhardt et al., 2017). It has been proposed that mass-flow deposits characterize sedimentation in the central basin, particularly at the foot of the northern and southern slopes and along the platform-edge delta fronts of the eastern margin (De Batist et al., 2002). Redeposition is indicated in our data by several proxies, in particular EM2 and the occurrence of framboidal pyrite (Raman spectroscopy; smear slides; not shown), vivianite (smear slides; not shown) and Mn maxima found at the steep slopes and in front of them. According to a shift from brownish sediment colors in the top ~2.5 cm of sediment cores IK 50 and 52 to greyish sediments below (not shown), the surface samples were taken from above the oxygen penetration depth (OPD), which is promoted by the oxygenated bottom water conditions in the lake (Karmanchuk, 2002). Such sediments should contain only marginal concentration of framboidal pyrite or vivianite, which require reducing conditions for their formation. On the other hand, Mn maxima occur particularly at the OPD, where mobilized Mn²⁺-ions in the anoxic pore water below meet oxygenated pore waters above. One potential explanation for the coincident occurrence of framboidal pyrite, vivianite and Mn maxima in the surface sediments of the deep, central basin could be mass wasting or turbidity currents. They may have transported pyrite, vivianite and dissolved manganese from subsurface sediments of more shallow sites downslope where they mix with the oxygen-rich lake water at the basin floor (Burdige, 1993; Naeyer et al., 2013). Consequently, increased Mn-oxide-mineralization may have occurred (Force & Cannon, 1988) leading to deposition of Mn-enriched sediments. Another explanation for the coincident occurrence of pyrite, vivianite and Mn maxima could be that small proportions of sediment from the OPD boundary have been included in sampling the surface sediments. Moreover, we cannot exclude that erosion may have removed oxygenated surface sediments at locations directly in front of the steep slopes. This might explain the slightly lower Mn concentrations directly in front of the southern slopes. Rapidly decreasing transport energies in front of basin slopes toward the center of the basin was observed, for example, at Lake El'gygytgyn (Juschus et al., 2009). In the gravity cores IK 50 and 52 from the more central basin, some thin (<2 cm) layers of mass waste deposits have been observed but no signs of erosion. Redeposition is presumably also the source of angular grains of sand, which can be observed in some samples from the deep central basin. The angular shape of these grains argues against aeolian input or long-distance fluvial transport and rather indicates short-distance transport, such as caused by debris-flow deposits. Such debris flow can emerge from collapsing slopes, partially develop into turbidites and can reach well into the basin (De Batist et al., 2002).

The spatial distribution of the Mn concentration suggests that redeposition is a dominant process along all slopes, with particularly long run-out distances across the southern and western basin floor. Although seismicity is proposed to be higher in the northern as compared to the southern part of the Issyk Kul basin (De Mol, 2006 and references therein; Figure 1 in Korzhenkov et al., 2022), the steep subaquatic slopes along the southern shore, together with potential meltwater pulses from glacially fed inlets and their sediment load, likely contribute to high EM2 (and also EM3 with minor proportions) values in the southern central basin (Figures 1, 2, and 5).

5.3. Authigenic Carbonate Production

SEM pictures and SEM data of idiomorphic calcite crystals together with the good correlation of TIC contents and Ca concentrations ($R^2 = 0.9$) suggest that the inorganic carbon fraction is mainly made up of fine-grained authigenic carbonates, more specifically calcium carbonates. Higher concentrations of Ca and TIC in the surface sediments as compared to the river samples (Figures 3 and 4) are consistent with an authigenic source. Carbonate is abundant in the surface sediments (<100 m water depth; ~25%), in particular in the central, deep basin (up to 60%). High TIC contents and Ca percentages in the deep central basin correlate with dominance of hemipelagic sedimentation (EM1) (Figures 2b and 9a) and a low quantity of siliciclastic material (Al, Fe, K, Ti, Rb, Si,

Zr; ~20%). This indicates that at these sites carbonate precipitation dominates over the accumulation of clastic sediments.

Petrological and SEM observations on cores IK 98-28 and IK 01-85, from the northern shelf area at ~200 m water depth, support that the carbonates composing the sediments are mainly authigenic (Giralt et al., 2002, 2004). The carbonates include several phases, that is, calcite, magnesian calcite, and monohydrocalcite (Rasmussen et al., 1996, 2000, 2001). Rasmussen et al. (2000) suggested that in cores IK 97-10P and IK 97-5P, recovered from ~230 to ~470 m water depth, respectively, carbonates make up 14–54% of the sediments, which is in agreement with our findings.

Generally, the presence of carbonate precipitates in the Issyk Kul sediments can be explained by the inflow of surface rivers and ground water enriched in Ca^{2+} and HCO_3^- ions (1.13–4.11 times supersaturated in CaCO_3) as a consequence of widespread calcareous bedrock in the Issyk Kul catchment (Karmanchuk, 2002; Morse & Mackenzie, 1990; Savvaitova & Petr, 1992). Precipitation of CaCO_3 likely occurs in the surface waters (epilimnion) and is generally triggered by higher water temperatures and cyanobacterial photosynthetic activity extracting CO_2 from those waters (e.g., Bosak, 2011; Leroy & Giralt, 2020). Summer temperatures in the epilimnion are around 20°C (Shabunin & Shabunin, 2002), which decreases CO_2 solubility in the water and influences the carbonate balance in the water column. However, temperatures are slightly higher in the peripheral zones of the lake compared to the colder central part. This would promote calcite precipitation in the peripheral zones, but contradicts partly with our observations. Also photosynthesis seems to be of minor importance for the calcite precipitation, as Issyk Kul is a hyperoligotrophic lake, with slightly increased productivity in the western and easternmost parts. The precipitates in the central part of Issyk Kul measure 2–3 μm on average and are transported, together with the detrital fine fraction, into the hypolimnion, such as reported from other lakes (e.g., Mischke et al., 2015; Roeser et al., 2021 and references therein). Supposedly, not all precipitated carbonate particles are deposited and preserved because of predictable dissolution in the hypolimnion due to undersaturation or a shift in pH of bottom water or pore water in surface sediments by CO_2 release from organic matter decomposition (e.g., Klump et al., 2020). Nonetheless, the good preservation of the rhombic carbonate crystals suggests that dissolution rates in the hypolimnion or at the sediment surface of Issyk Kul, like diatom dissolution (i-index averaging at 93%), are negligible.

Notably, carbonate precipitation in Issyk Kul is also a function of ion supply from the catchment and lake evaporation (Leroy et al., 2021; Morse & Mackenzie, 1990). In the Dzhergalan Bay, for more than 20 km from the river estuary, where surface water dilution by catchment glacial meltwaters leads to lowest salinity ($<5.8 \text{ g kg}^{-1}$) within the lake (Figure 2 in Zavialov et al., 2020), the formation of authigenic calcites is hindered. The same applies to the western shore, where the lake water is desalinated by the influx of ground waters (Romanovsky, 2002b). In contrast, the increased carbonate content in the northern part of the lake may be a function of relatively low dilution with freshwater, resulting in high salinity and ion concentration. From a geological perspective, similar observations have been made in other large lakes, where and when increased ion concentration led to increased calcite precipitation (e.g., Lake Ohrid; Francke et al., 2016). At Issyk Kul, published sediments cores dating back to the Pleistocene-Holocene transition indicate a similar pattern, with lower calcite precipitation during colder periods and/or during periods with increased freshwater supply (e.g., Leroy et al., 2021).

Whereas the pattern of calcite contents in the lake basin seems to be mainly controlled by salinity, the overall amount of calcite is probably triggered by the status of the lake as open- or closed-basin lake. High-resolution sedimentary records that allow a direct comparison of calcite precipitation and outlet activity over historical times are sparsely available to our knowledge. Giralt et al. (2004) present sediment core data of the last millennium, which show an increase in monohydrocalcite from values of around 30% to values of around 50% in the middle of the 18th century, when the outlet probably became inactive (Podrezov et al., 2020; Romanovsky, 2002a).

5.4. Biogenic Sedimentation

Overall, biogenic accumulation is low in Issyk Kul, as mirrored by relatively low concentrations of *n*-alkanes (averaging at $3.7 \mu\text{g g}^{-1}$ DW), alkenones (averaging at $0.4 \mu\text{g g}^{-1}$ DW) and TOC (averaging at 1.6%), except from the western extremity of the lake. In this context, concentrations of long-chain *n*-alkanes are interpreted as an indicator for terrestrial OM input, because *n*-alkanes display highest proportion from land plants, while concentrations of alkenones can be used as a measure of primary productivity within the lake. Because the biomarker

samples are few, the results have to be interpreted with caution. On the one hand, relatively low biogenic accumulation in Issyk Kul can be explained by generally low biomass production as a function of hyperoligotrophic conditions (Baetov, 2005). Poor supply of nutrients from the catchment is a result of restricted vegetation cover and relatively low river discharge as compared to total lake water mass (Savvaitova & Petr, 1992). On the other hand, high clastic input and water current energies in front of major river mouths along with wave action indicate dilution of OM by minerogenic matter and/or may prevent OM from settling (PCA axis 2; Figure 9a) (Meyers & Lallier-Vergés, 1999). This is particularly true for the Dzhergalan Bay where water inflow rates are highest (De Batist et al., 2002) and the bathymetry is steep (Podrezov et al., 2020).

In the western part of Issyk Kul (samples IK 8–10), elevated TOC contents (up to 6.4%) as well as partly elevated concentrations of *n*-alkanes and alkenones mirror increased OM deposition. In this shallow (<50 m), western, littoral zone resuspension of OM is lowest, river discharge is negligible (Savvaitova & Petr, 1992) and aquatic productivity is high. This is also indicated in highest amounts of N (NO_3 , NO_2 and NH_4) in the water column (Karmanchuk, 2002). High productivity is reflected by a dense cover of charophytes, the major component of aquatic vegetation in Issyk Kul, inhabiting water depths down to 40 m and spreading as far as 15 km offshore (Podrezov et al., 2020; Romanovsky, 2002b). In contrast to TOC and TN concentrations, *n*-alkanes and alkenones also display high concentrations in the Tyup Bay (IK 26), likely associated with highest LSTs at this site (Figures 7 and 8). Whereas most of the lake is hyperoligotrophic or oligotrophic, the Tyup Bay reached already mesotrophic conditions with suppression of macrophytes (Romanovsky, 2002b). Besides high aquatic productivity relatively low concentrations of clastic elements (SUM clastic) in the western part of Issyk Kul, indicate low minerogenic input from the catchment, which agrees with very low inflow rates (Savvaitova & Petr, 1992). Such low energies allow for OM (PCA axis 2; Figure 9a) and fine-grained material to settle and explain high proportions of hemipelagic sediments (EM1). They also favor good preservation of OM and diatom frustules (Figure 2).

An OM accumulation particularly in the south-western, shallow part of the lake instead of the entire western extremity of the lake may be associated with current-controlled nutrient availability or sediment refocusing. The western part of the lake is controlled by small-scale, local currents (Figure 2). Upwelling of nutrient enriched bottom waters in the westernmost part of the lake is promoted by the westerly winds prevailing in this lake area. However, easterly winds dominate in the easternmost part of the lake, promoting also upwelling in this area, and upwelling is also reported from the central part of the lake, where westerly and easterly winds, in combination with Coriolis force, lead to anticlockwise circulation (Figure 2; e.g., Shabunin & Shabunin, 2002). These local effects may have a large influence on OM distribution in the surface sediments.

PCA axis 2 indicates a depth-dependency of TOC/TN (Figure 9a). The depletion of TN relative to TOC with increasing water depth may be caused by selective decomposition of nitrogen, when the OM sinks all the way through the water column down to 668 m. The rate of decomposition of algal nitrogen is about twice as great as that of carbon (Otsuki & Hanya, 1972). Moreover, diagenetic loss of nitrogen after OM burial in the bottom sediments can elevate the TOC/TN ratio by up to 30–40% (Cohen, 2003). Nonetheless, CPI values (C_{27} – C_{31}) of >8.2 in all surface sediments of Issyk Kul indicate relatively fresh plant material (Eglinton & Hamilton, 1967; Meyers & Ishiwatari, 1993).

ACL values of around 30 in the western part of the lake and 29 in the eastern part may be associated with the dominantly semiarid climate and semidesert vegetation at the western part of the lake basin, while wetter climate allows for agricultural crop lands with belts of fruit trees along the shores of the eastern basin (Leroy & Giralt, 2020; Zhang et al., 2022; Figure 1). However, grasses and woody plants can produce highly variable but significant amounts of *n*-alkanes with chain lengths of C_{27} , C_{29} , C_{31} , and C_{33} (e.g., Bush & McInerney, 2013). This may explain the small difference between west and east.

Diatom growth in the open lake may be hampered by a deficit of soluble silica (Romanovsky, 2002b). Diatoms indicate the highest productivity in this western basin (78% of absolute diatom valve concentration; mostly benthic and facultative planktonic species), which agrees with earlier studies (Romanovsky, 2002b). Diatoms and, to a minor proportion, green algae can make up a considerable amount of the phytoplankton in Issyk Kul (Romanovsky, 2002b; Zhang et al., 2021). This is demonstrated by high abundances of diatom frustules (diatom valve concentrations) coinciding with high primary productivity (SUM alkenones), especially around IK 10. In this shallow area increased temperatures (Figures 6 and 7) together with ample nutrient supply from upwelling and ventilation of the lake waters by strong winds (Karmanchuk, 2002; Meyers & Lallier-Vergés, 1999; Orefice et al., 2019) likely favor aquatic productivity. Diatom valve concentration

may also depend on the trophic state in the individual areas of Lake Issyk Kul. The mesotrophic conditions with suppression of macrophytes in Tyup Bay (Romanovsky, 2002b) may promote diatom concentrations and may explain highest values of benthic diatoms in this part of the lake. Moreover, water analyses in the year 2016 showed highest concentration of silicates in the eastern part of the lake, which was attributed to supply of rivers Tyup and Jyrgalan (Zavialov et al., 2018) draining the granitoid bearing mountain ranges (e.g., De Grave et al., 2013). In addition to the supply of nutrients, also the pH may affect diatom growth and preservation in the lake, as pH of >9 have been measured in littoral parts of the lake in the period 1975–1993 (Karmanchuk, 2002). However, the *F*-index (see Figure S2 in Supporting Information S1) suggests that the littoral areas and areas <200 m, where highest pH values were measured in the water column, show better preservation of diatoms, which is probably related to lower calcite concentrations in the sediments from these areas.

5.5. Lake Surface and Air Temperatures

Both alkenone-based LST reconstructions (Müller et al., 1998; Prah1 et al., 1988) yield similar spatial variability (Figures 6 and 7) and average values ($13.3 \pm 0.5^\circ\text{C}$ and $13.6 \pm 1.0^\circ\text{C}$, including IK 58), which are slightly higher than the annual mean water temperature of 12.1°C measured at the meteorological station of Cholpon Ata (Figure 1) for the period 1972–2009 (Figure 7; Romanovsky et al., 2013). Slightly higher alkenone-based LST compared to measured water temperatures might be related to differing time intervals recorded, including an increase of water temperatures over the last decades (Romanovsky et al., 2013), but could also derive from higher phytoplankton productivity in spring or summer. In accordance with earlier findings (Romanovsky, 2002b; Shabunin & Shabunin, 2002), the spatial patterns display increased temperatures in the lake's western and eastern parts, especially the Rybachye and Tyup Bays, where shallow waters warm up more rapidly at times of insolation. In turn, temperatures decrease toward the lake center, where the water depth is high and upwelling causes a year-round cold-water dome (Romanovsky, 2002b; Shabunin & Shabunin, 2002). Several lake-specific calibrations exist for temperature reconstructions based on alkenones (Castañeda & Schouten, 2011), but none of them yielded reliable temperature estimates applicable for Issyk Kul. Although the here used alkenone-derived LST calibrations are based on haptophyte marine algae, that is, the marine coccolithophorid *Emiliana huxleyi* (Eglinton & Eglinton, 2008), they seem to reflect the measured temperatures quite accurately. One possible explanation may be that the group of alkenone-producing haptophyte algae in Issyk Kul are similar to those in marine settings (or dominated by a single species), because, after all, Issyk Kul is huge, saline, and oligotrophic much like the sea (Wang et al., 2016; Zavialov et al., 2020).

BrGDGT-based average MAT estimates (Peterse et al., 2012) seem to best reflect mean annual air temperatures of 8.3°C measured at Cholpon Ata for the period 1972–2009 (Figure 7; Romanovsky et al., 2013). In contrast, average MATs of 12.4°C using the global soil calibration of De Jonge et al. (2014) are closer to average mean summer temperatures (JJA; Figure 7). As microbial activity at this high elevation site is most likely restricted to the summer months, a warm-season bias is likely (Martinez Sosa et al., 2021; Raberg et al., 2021). However, MAF estimates using the global calibration for lake sediments (Raberg et al., 2021) overestimates measured MAF by about 5.4°C (Figure 7). The spatial MAT gradient with generally higher temperatures in the western shallow area and lower temperatures in the east is in agreement with weather station data, but differs from alkenone-derived LSTs (Figure 7). We therefore hypothesize that brGDGTs in the alkaline and slightly saline Issyk Kul are predominantly derived from erosion of soil in the catchment (Hopmans et al., 2004). However, we cannot exclude that some of the compounds are also produced in situ, that is, within the water column or the lake bottom sediments (Colcord et al., 2015; Loomis et al., 2014; Miller et al., 2018; Weber et al., 2015). Lack of fundamental knowledge on the identity and ecophysiology of the source organisms of brGDGTs, that is, the required redox state, nonetheless severely limits the interpretation (Loomis et al., 2014; Martinez Sosa et al., 2021; Miller et al., 2018; Weber et al., 2018), as does the relatively large calibration error for MAT estimates (De Jonge et al., 2014; Peterse et al., 2012).

5.6. Synopsis in View of Future Subsurface Sediment Studies

For prospective coring or drilling beyond existing Holocene records, the following observations are of key importance:

The recent generic origin of the sedimentary components is a function of water depth: nearshore deposition is mainly controlled by fluvial sediment supply of the clastic component, whereas in the deep basin authigenic carbonate production dominates (PCA axis 1; Figure 9a). These two major components (carbonate and clastic detritus; Figure 9b) show a negative correlation ($R^2 > 0.8$). Our findings are consistent with previous studies (De Batist et al., 2002; Giralt et al., 2004), which describe two main sedimentary provinces: (a) a terrigenous fraction mainly composed of siliciclastic minerals close to the shoreline and (b) an endogenic fraction mainly composed of calcium carbonates and clays in the deep central basin. Particularly high quantities of fluvial sediment supplied from eastern and southern tributaries suggest that sedimentation rates are relatively high at these shallow sites, but decrease basinward (Rasmussen et al., 2000).

Directional sediment transport by lake currents appears to be less important for the investigated proxies, except for the transport of very fine-grained organic matter. Redeposition of sediments seems to be a dominant process along all slopes, but is dominant at the basin floor only across its southern and western parts. Hence, our results suggest that remobilization of sediments does not dominate sedimentation in the central deep basin of Issyk Kul. Because several of our proxies (carbonate versus clastic fraction, grain-size distribution, TOC/TN, biomarker and diatom data, biomarker-inferred temperature reconstruction) as well as the PCA demonstrate a depth-dependency, sediments in the central basin are likely deposited in situ. Consequently, older sediments in the deep basin are likely produced in situ, though they also include some redeposited material (De Batist et al., 2002). A core from the central deep basin should therefore reach the oldest stratigraphic ranges and offer a widely undisturbed sedimentary succession for palaeoenvironmental reconstructions.

5.6.1. Future Core Data and Proxies Should Consider the Following Conclusions

It may be possible to identify changing influences of different sediment provinces using the variability in the mineralogical data. According to our EDXRF and PCA data, the clastic component shows two groupings: Fe, Ti, Zr and Al, Si, Rb, K, with the latter group discriminating river input from the Dzhergalan. Sediment discharge from the Chu River, which entered Issyk Kul at its western end until the late Pleistocene, may be determined by a distinct change in mineralogy at that time. Because of the complex catchment geology, further distinctions may be difficult. Direct input from local glaciers during the last glacial period (Grosswald et al., 1994) has certainly modified the mineralogical composition and has presumably supplied coarse-grained (fine-grained) material to nearshore (central lake) areas.

Down-core shifts in the generic origin of the sedimentary components, for example, clastic-versus carbonate-driven sedimentation in the central basin, may capture long-term climatic changes with a predominantly terrigenous source during cold, glacial stages and high authigenic carbonate production during warm interglacial periods. A similar correlation has, for example, been observed in the record from ancient Lake Ohrid (Francke et al., 2016). This is also observed in sediment records from Issyk Kul and can also be related to the status of the lake as open-basin or closed-basin lake (e.g., Leroy et al., 2021).

Changes in lake ecology, temperatures, and catchment vegetation can be inferred from diatom and biomarker data, because preservation is good, even at great depths. Drastic changes in water level may be evident in proxies, which show a strong depth-dependency, that is, carbonate versus clastic fraction, grain-size distribution, TOC/TN, biomarker and diatom data, or lake temperatures. For example, a significantly lower water level should result in rivers discharging coarse-grained sediment much further into the lake's central basin. Remobilization of shallow-water sediments into the deep basin of Issyk Kul, due to for example, lake-level changes or seismicity may be identifiable by high Mn, high amounts of the coarse-grained, clastic fraction and benthic or facultative benthic diatoms in the deep central basin. Because Fe has mainly a detrital source and Mn is mainly driven by named redeposition processes, Fe/Mn ratios seem to be not applicable as proxy for redox conditions, as used before in other deep and old lakes (e.g., Melles et al., 2012).

6. Conclusions

A quasi-equidistant sampling grid of up to 66 sediment surface (and 10 river) samples spanning the entire lake basin of Issyk Kul, Kyrgyzstan, was examined by means of a multiproxy approach combining (bio)geochemical, granulometric and microscopic analyses and statistical methods. The data add important spatial information on the major physical, chemical and biological processes controlling modern sedimentation patterns in Issyk Kul.

- Highest quantities of fluvial sediments are deposited nearshore, in particular by the high-energetic, eastern tributaries. Distinct differences in riverine sediment supply are, moreover, recorded between the northern and southern tributaries, likely as a result of higher uplift and erosion rates in the south and far greater glaciation extent in the Terskey Alatau compared to the opposite Kungey Alatau Range.
- Toward the center of the lake, the endogenic sediment fraction is mainly composed of calcium carbonates, which form in the epilimnion and precipitate out on the deep basin floor. Organic endogenic sediments show an alteration that is partly triggered to the large depth of the lake.
- Biogenic sedimentation is overall low compared to clastic input and mainly restricted to the western, shallow extremity of the lake, where the nearshore, shallow-water, low-energetic environment favors aquatic productivity, organic material deposition, and preservation.
- Directional sediment transport by lake currents appears to be of minor importance for the investigated proxies, except for the transport of very fine-grained organic matter.
- Redeposition appears to be a dominant process along the slopes and across the southern and western basin floor. In addition, wave action affects sedimentation in the shallower areas of up to several tens of meters water depth.
- Given that the Chu River delivered significant sediment discharge into Issyk Kul at its western end until the late Pleistocene, a long, continuous depositional history may be reached only in the central deep basin.
- Alkenones are promising biomarkers for reconstructing lake surface temperatures and primary productivity.

Conflict of Interest

The authors declare no conflicts of interest relevant to this study.

Data Availability Statement

All data used for this study are available at the Zenodo data repository via <https://doi.org/10.5281/zenodo.8059855> (Lenz et al., 2023) after publication.

Acknowledgments

The research project was supported by the Deutsche Forschungsgemeinschaft (WA2109/18). We are grateful for the support of our local partners in Kyrgyzstan, particularly the crew of RV Moltur, for their logistical help during the fieldwork. We like to thank N. Mantke, J. Feller, H. Cieszynski, and B. Stapper from the University of Cologne for their assistance during laboratory work. The reviewers Julie Brigham-Grette, Thomas C. Johnson, and an anonymous reviewer provided very valuable comments and suggestions to improve the manuscript. Open Access funding enabled and organized by Projekt DEAL.

References

- Aizen, V. B., Aizen, E. M., & Melack, J. M. (1995). Climate, snow cover, glaciers, and runoff in the Tien Shan, Central Asia. *Journal of The American Water Resources Association, Water Resources Bulletin*, 31(6), 1113–1129. <https://doi.org/10.1111/j.1752-1688.1995.tb03426.x>
- Albrecht, C., & Wilke, T. (2008). Ancient Lake Ohrid: Biodiversity and evolution. *Hydrobiologia*, 615(1), 103–140. <https://doi.org/10.1007/s10750-008-9558-y>
- Alifujiang, Y., Abuduwaili, J., Groll, M., Issanova, G., & Maihemuti, B. (2021). Changes in intra-annual runoff and its response to climate variability and anthropogenic activity in the Lake Issyk-Kul Basin, Kyrgyzstan. *Catena*, 198, 104974. <https://doi.org/10.1016/j.catena.2020.104974>
- Baetov, R. (2005). Lake Issyk-Kul. In *Managing lakes and their basins for sustainable future* (pp. 193–204). International Lake Environment Committee Foundation.
- Battarbee, R. W., Jones, V. J., Flower, R. J., Cameron, N. G., Bennion, H., Carvalho, L., et al. (2001). Diatoms. In J. P. Smol, H. J. B. Briks, & W. M. Last (Eds.), *Tracking environmental change using lake sediments. Volume 3: Terrestrial, algal, and siliceous indicators* (pp. 155–202). Kluwer Academic Publishers.
- Blott, S. J., & Pye, K. (2001). Gradistat: A grain size distribution and statistics package for the analysis of unconsolidated sediments. *Earth Surface Processes and Landforms*, 26(11), 1237–1248. <https://doi.org/10.1002/esp.261>
- Bosak, T. (2011). Calcite precipitation, microbially Induced. In J. Reitner, & V. Thiel (Eds.), *Encyclopedia of geobiology. Encyclopedia of earth sciences series* (pp. 223–227). Springer. https://doi.org/10.1007/978-1-4020-9212-1_41
- Bray, E., & Evans, E. (1961). Distribution of n-paraffins as a clue to recognition of source beds. *Geochimica et Cosmochimica Acta*, 22(1), 2–15. [https://doi.org/10.1016/0016-7037\(61\)90069-2](https://doi.org/10.1016/0016-7037(61)90069-2)
- Bro, R., & Smilde, A. K. (2014). Principal component analysis. *Analytical Methods*, 6(9), 2812–2831. <https://doi.org/10.1039/C3AY41907J>
- Burdige, D. J. (1993). The biogeochemistry of manganese and iron reduction in marine sediments. *Earth-Science Reviews*, 35(3), 249–284. [https://doi.org/10.1016/0012-8252\(93\)90040-E](https://doi.org/10.1016/0012-8252(93)90040-E)
- Burgette, R. J., Weldon, R. J., Abdrakhmatov, K. Y., Ormukov, C., Owen, L. A., & Thompson, S. C. (2017). Timing and process of river and lake terrace formation in the Kyrgyz Tien Shan. *Quaternary Science Reviews*, 159, 15–34. <https://doi.org/10.1016/j.quascirev.2017.01.003>
- Bush, R. T., & McNerney, F. A. (2013). Leaf wax n-alkane distributions in and across modern plants: Implications for paleoecology and chemotaxonomy. *Geochimica et Cosmochimica Acta*, 117, 161–179. <https://doi.org/10.1016/j.gca.2013.04.016>
- Castañeda, I. S., & Schouten, S. (2011). A review of molecular organic proxies for examining modern and ancient lacustrine environments. *Quaternary Science Reviews*, 30(21–22), 2851–2891. <https://doi.org/10.1016/j.quascirev.2011.07.009>
- Ceramicola, S., Rebescio, M., De Batist, M., & Khlystov, O. (2001). Seismic evidence of small-scale lacustrine drifts in Lake Baikal (Russia). *Marine Geophysical Researches*, 22(5), 445–464. <https://doi.org/10.1023/A:1016351700435>
- Chedia, O. K. (1986). *Morphology and neotectonics of the tien Shan* (in Russian) (p. 313). Ilim Publications.
- Cohen, A. S. (2003). *Paleolimnology: The history and evolution of Lake systems* (p. 528). Oxford University Press.

- Colcord, D. E., Cadieux, S. B., Brassell, S. C., Castañeda, I. S., Pratt, L. M., & White, J. R. (2015). Assessment of branched GDGTs as temperature proxies in sedimentary records from several small lakes in southwestern Greenland. *Organic Geochemistry*, 82, 33–41. <https://doi.org/10.1016/j.orggeochem.2015.02.005>
- De Batist, M., Imbo, Y., Vermeesch, P., Klerkx, J., Giralt, S., Delvaux, D., et al. (2002). Bathymetry and sedimentary environments of Lake Issyk-Kul, Kyrgyz Republic (central Asia): A large, high-altitude, tectonic lake. In J. Klerkx, & B. Imanackunov (Eds.), *Lake Issyk-Kul: Its natural environment* (pp. 101–124). Kluwer Academic Publishers.
- De Grave, J., Glorie, S., Buslov, M. M., Stockli, D. F., McWilliams, M. O., Batalev, V. Y., et al. (2013). Thermo-tectonic history of the Issyk-Kul basin (Kyrgyz northern tien Shan, central Asia). *Gondwana Research*, 23(3), 998–1020. <https://doi.org/10.1016/j.gr.2012.06.014>
- De Jonge, C., Hopmans, E. C., Zell, C. I., Kim, J. H., Schouten, S., & Sinninghe Damsté, J. S. (2014). Occurrence and abundance of 6-methyl branched glycerol dialkyl glycerol tetraethers in soils: Implications for palaeoclimate reconstruction. *Geochimica et Cosmochimica Acta*, 141, 97–112. <https://doi.org/10.1016/j.gca.2014.06.013>
- De Mol, L. (2006). *Reconstructie van meerspiegelschommelingen in het Issyk-Kul Meer (Kirgizie) op basis van de geomorfologische en seismostratigrafische analyse van rivierdelta's* (Master). University of Gent.
- Dikich, A. N. (2004). *Gletscherwasserressourcen der Issyk-Kul-Region (Kirgistan), ihr gegenwärtiger und zukünftiger Zustand* (Discussion Paper No. 19). Justus Liebig University Giessen. Retrieved from <http://hdl.handle.net/10419/21890>
- Eglinton, T. I., & Eglinton, G. (2008). Molecular proxies for paleoclimatology. *Earth and Planetary Science Letters*, 275(1), 1–16. <https://doi.org/10.1016/j.epsl.2008.07.012>
- Eglinton, G., & Hamilton, R. J. (1967). Leaf epicuticular waxes. *Science*, 156(3780), 1322–1335. <https://doi.org/10.1126/science.156.3780.1322>
- Ficken, K. J., Li, B., Swain, D., & Eglinton, G. (2000). An *n*-alkane proxy for the sedimentary input of submerged/floating freshwater aquatic macrophytes. *Organic Geochemistry*, 31(7–8), 745–749. [https://doi.org/10.1016/S0146-6380\(00\)00081-4](https://doi.org/10.1016/S0146-6380(00)00081-4)
- Force, E. R., & Cannon, W. F. (1988). Depositional model for shallow-marine manganese deposits around black shale basins. *Economic Geology*, 83(1), 93–117. <https://doi.org/10.2113/gsecongeo.83.1.93>
- Francke, A., Wagner, B., Just, J., Leicher, N., Gromig, R., Baumgarten, H., et al. (2016). Sedimentological processes and environmental variability at Lake Ohrid (Macedonia, Albania) between 637 ka and the present. *Biogeosciences*, 13(4), 1179–1196. <https://doi.org/10.5194/bg-13-1179-2016>
- Francke, A., Wagner, B., Leng, M., & Rethemeyer, J. (2013). A Late Glacial to Holocene record of environmental and human variability derived from a sediment record from Lake Dojran (Macedonia, Greece). *Climate of the Past*, 9(1), 481–498. <https://doi.org/10.5194/cp-9-481-2013>
- Gebhardt, A. C., Naudts, L., De Mol, L., Klerkx, J., Abdrakhmatov, K., Sobel, E. R., et al. (2017). High-amplitude lake-level changes in tectonically active Lake Issyk-Kul (Kyrgyzstan) revealed by high-resolution seismic reflection data. *Climate of the Past*, 13(1), 73–92. <https://doi.org/10.5194/cp-13-73-2017>
- Giralt, S., Julià, R., Klerkx, J., Riera, S., Leroy, S., Buchaca, T., et al. (2004). 1,000-Year environmental history of Lake Issyk-Kul. In J. C. J. Nihoul, P. O. Zavialov, & P. P. Micklin (Eds.), *Dying and dead seas: Climatic versus anthropic causes* (pp. 253–285). Kluwer Academic Publishers.
- Giralt, S., Klerkx, J., Riera, S., Julia, R., Lignier, V., Beck, C., et al. (2002). Recent Paleoenvironmental evolution of Lake Issyk-Kul. In J. Klerkx, & B. Imanackunov (Eds.), *Lake Issyk-Kul: Its natural environment* (pp. 125–146). Kluwer Academic Publishers.
- Gómez-Paccard, M., Larrasoana, J. C., Giralt, S., & Roberts, A. P. (2012). First paleomagnetic results of mid-to late Holocene sediments from Lake Issyk-Kul (Kyrgyzstan): Implications for paleosecular variation in central Asia. *Geochemistry, Geophysics, Geosystems*, 13, Q03019. <https://doi.org/10.1029/2011GC004015>
- Grosswald, M., Kuhle, M., & Fastook, J. (1994). Würm glaciation of Lake Issyk-Kul area, tian Shan Mts.: A case study in glacial history of central Asia. *Geojournal*, 33(2), 273–310. <https://doi.org/10.1007/BF00812878>
- Håkanson, L. (1977). The influence of wind, fetch, and water depth on the distribution of sediments in Lake Vänern, Sweden. *Canadian Journal of Earth Sciences*, 14(3), 397–412. <https://doi.org/10.1139/e77-040>
- Hammer, O., Harper, D. A. T., & Ryan, P. D. (2001). Past: Paleontological statistics software package for education and data analysis. *Palaentologica Electronica*, 4(1), 9.
- Hasberg, A. K. M., Bijaksana, S., Held, P., Just, J., Melles, M., Morlock, M. A., et al. (2019). Modern sedimentation processes in Lake Towuti, Indonesia, revealed by the composition of surface sediments. *Sedimentology*, 66(2), 675–698. <https://doi.org/10.1111/sed.12503>
- Hofer, M., Peeters, F., Aeschbach-Hertig, W., Brennwald, M., Holoher, J., Livingstone, D. M., et al. (2002). Rapid deep-water renewal in Lake Issyk-Kul (Kyrgyzstan) indicated by transient tracers. *Limnology & Oceanography*, 47(4), 1210–1216. <https://doi.org/10.4319/lo.2002.47.4.1210>
- Hopmans, E. C., Schouten, S., & Sinninghe Damsté, J. S. (2016). The effect of improved chromatography on GDGT-based palaeoproxies. *Organic Geochemistry*, 93, 1–6. <https://doi.org/10.1016/j.orggeochem.2015.12.006>
- Hopmans, E. C., Weijers, J. W. H., Schefuß, E., Herfort, L., Sinninghe Damsté, J. S., & Schouten, S. (2004). A novel proxy for terrestrial organic matter in sediments based on branched and isoprenoid tetraether lipids. *Earth and Planetary Science Letters*, 224(1), 107–116. <https://doi.org/10.1016/j.epsl.2004.05.012>
- Johnson, T. C. (1980). Sediment redistribution by waves in lakes, reservoirs and embayments. In H. Stefan (Ed.), *Proceedings of the symposium of surface water impoundments* (pp. 1307–1317). American Society of Civil Engineers.
- Juscius, O., Melles, M., Gebhardt, A. C., & Niessen, F. (2009). Late quaternary mass movement events in Lake El'gygytyn, north-eastern Siberia. *Sedimentology*, 56(7), 2155–2174. <https://doi.org/10.1111/j.1365-3091.2009.01074.x>
- Karmanchuk, A. S. (2002). Water chemistry and ecology of Lake Issyk-Kul. In J. Klerkx, & B. Imanackunov (Eds.), *Lake Issyk-Kul: Its natural environment* (pp. 13–26). Kluwer Academic Publishers.
- Kipfer, R., & Peeters, F. (2002). Using transient conservative and environmental tracers to study water exchange in Lake Issyk-Kul. In J. Klerkx, & B. Imanackunov (Eds.), *Lake Issyk-Kul: Its natural environment* (pp. 89–100). Kluwer Academic Publishers.
- Klump, J. V., Edgington, D. N., Granina, L., & Remsen, C. C. (2020). Estimates of the remineralization and burial of organic carbon in Lake Baikal sediments. *Journal of Great Lakes Research*, 46(1), 102–114. <https://doi.org/10.1016/j.jglr.2019.10.019>
- Korzhenkov, A. M., & Deev, E. V. (2017). Underestimated seismic hazard in the south of the Issyk-Kul Lake region (northern Tian Shan). *Geodesy and Geodynamics*, 8(3), 169–180. <https://doi.org/10.1016/j.geog.2017.03.012>
- Korzhenkov, A. M., Deev, E. V., Korzhenkova, L. A., Liu, J., Mažeika, Y. V., Rogozhin, E. A., et al. (2022). Strong seismic activity of the Terskey Ala-Too range Adyrs, northern tien Shan, in the Holocene from radiocarbon analysis data. *Izvestiya—Physics of the Solid Earth*, 58(2), 243–266. <https://doi.org/10.1134/S1069351322010049>
- Krammer, K., & Lange-Bertalot, H. (1986). *Bacillariophyceae. Teil 1: Naviculaceae*. Gustav Fischer Verlag.
- Krammer, K., & Lange-Bertalot, H. (1988). *Bacillariophyceae. Teil 2: Bacillariaceae, Epithemiaceae, Surirellaceae*. Gustav Fischer Verlag.
- Krammer, K., & Lange-Bertalot, H. (1991a). *Bacillariophyceae. Teil 3: Centrales, Fragilariaceae, Eunotiaceae*. Gustav Fischer Verlag.

- Krammer, K., & Lange-Bertalot, H. (1991b). *Bacillariophyceae. Teil 4: Achmanthaceae, Kritische Ergänzungen zu Navicula (Lineolatae) und Gomphonema*. Gustav Fischer Verlag.
- Krivoshel, M. I., & Granskaya, T. P. (1986). Water balance of Lake Issyk Kul (in Russian). In A. V. Shnitnikov (Ed.), *Studies of large lakes in the USSR* (pp. 276–280). Nauka.
- Larrasoña, J. C., Gómez-Paccard, M., Giralt, S., & Roberts, A. P. (2011). Rapid locking of tectonic magnetic fabrics in weakly deformed mudrocks. *Tectonophysics*, *507*(1), 16–25. <https://doi.org/10.1016/j.tecto.2011.05.003>
- Lenz, M. M., Scheuer, R., Zhang, X., Jaeschke, A., Opitz, S., Leicher, N., et al. (2023). Modern sedimentation patterns in Lake Issyk Kul (Kyrgyzstan), derived from surface sediment and inlet stream samples [Dataset]. Zenodo. <https://doi.org/10.5281/zenodo.8059855>
- Leroy, S. A. G., & Giralt, S. R. (2020). Humid and cold periods in the last 5600 years in Arid Central Asia revealed by palynology of *Picea schrenkiana* from Issyk-Kul. *The Holocene*, *31*(3), 380–391. <https://doi.org/10.1177/0959683620972776>
- Leroy, S. A. G., Ricketts, R. D., & Rasmussen, K. A. (2021). Climatic and limnological changes 12,750 to 3600 years ago in the Issyk-Kul catchment, Tien Shan, based on palynology and stable isotopes. *Quaternary Science Reviews*, *259*, 106897. <https://doi.org/10.1016/j.quascirev.2021.106897>
- Li, Q., Wu, J., Zhou, J., Sakiev, K., & Hofmann, D. (2020). Occurrence of polycyclic aromatic hydrocarbon (PAH) in soils around two typical lakes in the western Tian Shan Mountains (Kyrgyzstan, Central Asia): Local burden or global distillation? *Ecological Indicators*, *108*, 105749. <https://doi.org/10.1016/j.ecolind.2019.105749>
- Li, Y., Ma, L., Abuduwaili, J., Li, Y., & Abdyzhapar uulu, S. (2022). Spatiotemporal distributions of fluoride and arsenic in rivers with the role of mining industry and related human health risk assessments in Kyrgyzstan. *Exposure and Health*, *14*(1), 49–62. <https://doi.org/10.1007/s12403-021-00417-5>
- Liu, W., Ma, L., Li, Y., Abuduwaili, J., & Abdyzhapar uulu, S. (2020). Heavy metals and related human health risk assessment for river waters in the Issyk-Kul basin, Kyrgyzstan, central Asia. *International Journal of Environmental Research and Public Health*, *17*(10), 3506. <https://doi.org/10.3390/ijerph17103506>
- Loomis, S. E., Russell, J. M., Heureux, A. M., D'Andrea, W. J., & Sinninghe Damsté, J. S. (2014). Seasonal variability of branched glycerol dialkyl glycerol tetraethers (brGDGTs) in a temperate lake system. *Geochimica et Cosmochimica Acta*, *144*, 173–187. <https://doi.org/10.1016/j.gca.2014.08.027>
- Martinez Sosa, P., Tierney, J., Stefanescu, I. C., Crampton-Flood, E. D., Shuman, B. N., & Routsom, C. (2021). A global Bayesian temperature calibration for lacustrine brGDGTs. *Geochimica et Cosmochimica Acta*, *305*, 87–105. <https://doi.org/10.1016/j.gca.2021.04.038>
- Melles, M., Brigham-Grette, J., Minyuk, P. S., Nowaczyk, N. R., Wennrich, V., DeConto, R. M., et al. (2012). 2.8 million years of Arctic climate change from Lake El'gygytgyn, NE Russia. *Science*, *337*(6092), 315–320. <https://doi.org/10.1126/science.1222135>
- Merkel, B. J., & Kulenbekov, Z. (2012). Investigation of the natural uranium content in the Issyk-Kul Lake, Kyrgyzstan. *Freiberg Online Geology*, *33*, 3–45.
- Meyers, P. A., & Ishiwatari, R. (1993). Lacustrine organic geochemistry—An overview of indicators of organic matter sources and diagenesis in lake sediments. *Organic Geochemistry*, *20*(7), 867–900. [https://doi.org/10.1016/0146-6380\(93\)90100-P](https://doi.org/10.1016/0146-6380(93)90100-P)
- Meyers, P. A., & Lallier-Vergés, E. (1999). Lacustrine sedimentary organic matter records of late quaternary paleoclimates. *Journal of Paleolimnology*, *21*(3), 345–372. <https://doi.org/10.1023/A:1008073732192>
- Meyers, P. A., & Terranes, J. L. (2001). Sediment organic matter. In W. M. Last, & J. P. Smol (Eds.), *Tracking environmental change using lake sediments, volume 2: Physical and geo-chemical methods* (pp. 239–269). Springer.
- Miller, D. R., Habicht, M. H., Keisling, B. A., Castañeda, I. S., & Bradley, R. S. (2018). A 900-year New England temperature reconstruction from in situ seasonally produced branched glycerol dialkyl glycerol tetraethers (brGDGTs). *Climate of the Past*, *14*(11), 1653–1667. <https://doi.org/10.5194/cp-14-1653-2018>
- Mischke, S., Opitz, S., Kalbe, J., Ginat, H., & Al-Saqarat, B. (2015). Palaeoenvironmental inferences from late quaternary sediments of the Al Jafr basin, Jordan. *Quaternary International*, *382*, 154–167. <https://doi.org/10.1016/j.quaint.2014.12.041>
- Molnar, P., & Tapponnier, P. (1975). Cenozoic tectonics of Asia: Effects of a continental collision. *Science*, *189*(4201), 419–426. <https://doi.org/10.1126/science.189.4201.419>
- Morse, J. W., & Mackenzie, F. T. (1990). *Geochemistry of sedimentary carbonates*. Elsevier.
- Müller, P. J., Kirst, G., Ruhland, G., von Storch, I., & Rosell-Melé, A. (1998). Calibration of the alkenone paleotemperature index U_{37K'} based on core-tops from the eastern South Atlantic and the global ocean (60°N–60°S). *Geochimica et Cosmochimica Acta*, *62*(10), 1757–1772. [https://doi.org/10.1016/S0016-7037\(98\)00097-0](https://doi.org/10.1016/S0016-7037(98)00097-0)
- Naeher, S., Gilli, A., North, R. P., Hamann, Y., & Schubert, C. J. (2013). Tracing bottom water oxygenation with sedimentary Mn/Fe ratios in Lake Zurich, Switzerland. *Chemical Geology*, *352*, 125–133. <https://doi.org/10.1016/j.chemgeo.2013.06.006>
- Oberhänsli, H., & Molnar, P. (2012). Climate evolution in central Asia during the past few million Years: A case study from Issyk Kul. *Scientific Drilling*, *13*, 51–57. <https://doi.org/10.2204/iodp.sd.13.09.2011>
- Orefice, I., Musella, M., Smerilli, A., Sansone, C., Chandrasekaran, R., Corato, F., et al. (2019). Role of nutrient concentrations and water movement on diatom's productivity in culture. *Scientific Reports*, *9*(1), 1479. <https://doi.org/10.1038/s41598-018-37611-6>
- Otsuki, A., & Hanya, T. (1972). Production of dissolved organic matter from dead green algal cells. I. Aerobic microbial decomposition. *Limnology & Oceanography*, *17*(2), 248–257. <https://doi.org/10.4319/lo.1972.17.2.0248>
- Paterson, G. A., & Heslop, D. (2015). New methods for unmixing sediment grain size data. *Geochemistry, Geophysics, Geosystems*, *16*, 4494–4506. <https://doi.org/10.1002/2015GC006070>
- Peeters, F., Finger, D., Hofer, M., Brennwald, M., Livingstone, D. M., & Kipfer, R. (2003). Deep-water renewal in Lake Issyk-Kul driven by differential cooling. *Limnology & Oceanography*, *48*(4), 1419–1431. <https://doi.org/10.4319/lo.2003.48.4.1419>
- Peterse, F., van der Meer, J., Schouten, S., Weijers, J. W. H., Fierer, N., Jackson, R. B., et al. (2012). Revised calibration of the MBT-CBT paleotemperature proxy based on branched tetraether membrane lipids in surface soils. *Geochimica et Cosmochimica Acta*, *96*, 215–229. <https://doi.org/10.1016/j.gca.2012.08.011>
- Podrezov, A. O., Mäkelä, A. J., & Mischke, S. (2020). Lake Issyk-Kul: Its history and present state. In S. Mischke (Ed.), *Large Asian lakes in a changing world. Natural state and human impact* (pp. 177–206). Springer Water.
- Prahl, F. G., Muehlhausen, L. A., & Zahnle, D. L. (1988). Further evaluation of long-chain alkenones as indicators of paleoceanographic conditions. *Geochimica et Cosmochimica Acta*, *52*(9), 2303–2310. [https://doi.org/10.1016/0016-7037\(88\)90132-9](https://doi.org/10.1016/0016-7037(88)90132-9)
- Prahl, F. G., & Wakeham, S. G. (1987). Calibration of unsaturation patterns in long-chain ketone compositions for palaeotemperature assessment. *Nature*, *330*(6146), 367–369. <https://doi.org/10.1038/330367a0>
- Raberg, J. H., Harning, D. J., Crump, S. E., De Wet, G., Blumm, A., Kopf, S., et al. (2021). Revised fractional abundances and warm-season temperatures substantially improve brGDGT calibrations in lake sediments. *Biogeosciences*, *18*(12), 3579–3603. <https://doi.org/10.5194/bg-18-3579-2021>

- Rasmussen, K. A., Ricketts, R. D., Johnson, T. C., Romanovsky, V. V., & Grigina, O. M. (2000). An 11,000-year history of central Asian Paleoclimate change recorded in deep sediments of Lake Issyk-Kul, Kyrgyzstan (Abstract). Paper presented at the Abstracts of the American Geophysical Union Fall Meeting, San Francisco, CA, 81, F657.
- Rasmussen, K. A., Ricketts, R. D., Johnson, T. C., Romanovsky, V. V., & Grigina, O. M. (2001). An 8,000 Year multi-proxy record from Lake Issyk-Kul, Kyrgyzstan. *PAGES News*, 9(2), 5–6. <https://doi.org/10.22498/pages.9.2.5>
- Rasmussen, K. A., Romanovsky, V. V., & MacIntyre, I. G. (1996). Late Quaternary coastal microbialites and beachrocks of Lake Issyk-Kul, Kyrgyzstan: Geologic, hydrographic, and climatic significance (Abstract). (Vol. 28). Paper presented at the Geological Society of America. Annual Meeting, Abstracts with Programs. A-304.
- Reimer, A., Landmann, G., & Kempe, S. (2009). Lake van, eastern Anatolia, hydrochemistry and history. *Aquatic Geochemistry*, 15(1), 195–222. <https://doi.org/10.1007/s10498-008-9049-9>
- Ricketts, R. D., Johnson, T. C., Brown, E. T., Rasmussen, K. A., & Romanovsky, V. V. (2001). The Holocene paleolimnology of Lake Issyk-Kul, Kyrgyzstan: Trace element and stable isotope composition of ostracodes. *Palaeogeography, Palaeoclimatology, Palaeoecology*, 176(1), 207–227. [https://doi.org/10.1016/S0031-0182\(01\)00339-X](https://doi.org/10.1016/S0031-0182(01)00339-X)
- Roeser, P., Dräger, N., Brykala, D., Ott, F., Pinkerneil, S., Gierszewski, P., et al. (2021). Advances in understanding calcite varve formation: New insights from a dual lake monitoring approach in the southern Baltic lowlands. *Boreas*, 50(2), 419–440. <https://doi.org/10.1111/bor.12506>
- Rojas-Jimenez, K., Araya-Lobo, A., Quesada-Perez, F., Akerman-Sanchez, J., Delgado-Duran, B., Ganzert, L., et al. (2021). Variation of bacterial communities along the vertical gradient in Lake Issyk Kul, Kyrgyzstan. *Environmental Microbiology Reports*, 13(3), 337–347. <https://doi.org/10.1111/1758-2229.12935>
- Romanovsky, V. V. (1990). *The natural complex of Lake Issyk-Kul (in Russian)*. Academy Nauk Kyrgyzstan.
- Romanovsky, V. V. (2002a). Water level variations and water balance of Lake Issyk-Kul. In J. Klerkx, & B. Imanackunov (Eds.), *Lake Issyk-Kul: Its natural environment* (pp. 45–57). Kluwer Academic Publishers.
- Romanovsky, V. V. (2002b). Hydrobiology of Lake Issyk-Kul. In J. Klerkx, & B. Imanackunov (Eds.), *Lake Issyk-Kul: Its natural environment* (pp. 27–44). Kluwer Academic Publishers.
- Romanovsky, V. V., & Shabunin, G. D. (2002). Currents and vertical water exchange in Lake Issyk Kul. In J. Klerkx, & B. Imanackunov (Eds.), *Lake Issyk-Kul: Its natural environment* (pp. 77–87). Kluwer Academic Publishers.
- Romanovsky, V. V., Tashbaeva, S., Crétaux, J. F., Calmant, S., & Drolon, V. (2013). The closed Lake Issyk-Kul as an indicator of global warming in Tien-Shan. *Natural Science*, 5(05), 608–623. <https://doi.org/10.4236/ns.2013.55076>
- Rosenwinkel, S., Landgraf, A., Schwanghart, W., Volkmer, F., Dzhumabaeva, A., Merchel, S., et al. (2017). Late Pleistocene outburst floods from Issyk Kul, Kyrgyzstan? *Earth Surface Processes and Landforms*, 42(10), 1535–1548. <https://doi.org/10.1002/esp.4109>
- Roud, S. C., Wack, M. R., Gilder, S. A., Kudriavtseva, A., & Sobel, E. R. (2021). Miocene to early Pleistocene depositional history and tectonic evolution of the Issyk-Kul basin, central tian Shan. *Geochemistry, Geophysics, Geosystems*, 22, e2020GC009556. <https://doi.org/10.1029/2020GC009556>
- Ryves, D. B., Juggins, S., Fritz, S. C., & Battarbee, R. W. (2001). Experimental diatom dissolution and the quantification of microfossil preservation in sediments. *Paleogeography, Paleoclimatology, Paleoecology*, 172(1–2), 99–113. [https://doi.org/10.1016/S0031-0182\(01\)00273-5](https://doi.org/10.1016/S0031-0182(01)00273-5)
- Savvaivaita, K., & Petr, T. (1992). Lake Issyk-Kul, Kirgizia. *International Journal of Salt Lake Research*, 1(2), 21–46. <https://doi.org/10.1007/BF02904361>
- Sevastyanov, D. V., & Smirnova, N. P. (1986). Lake Issyk-kul and trends in its natural development (in Russian). Nauka.
- Shabunin, G. D., & Shabunin, A. G. (2002). Climate and physical properties of water in Lake Issyk-Kul. In J. Klerkx, & B. Imanackunov (Eds.), *Lake Issyk-Kul: Its natural environment* (pp. 3–11). Kluwer Academic Publishers.
- Team, Q. D. (2022). QGIS Geographic information system. Open Source. Geospatial Foundation Project. Retrieved from <http://qgis.osgeo.org>
- The MathWorks Inc. (2021). *MATLAB version 9.11.0.1751886 (Version R2021b)*. The MathWorks Inc.
- Trofimov, A. K. (1990). *Quaternary deposits of Issyk-Kul Basin in connection to its tectonics* (in Russian) (Vol. N1). Izvestia A.S. Kirghyzkoy SSR.
- Vogel, H., Wessels, M., Albrecht, C., Stich, H. B., & Wagner, B. (2010). Spatial variability of recent sedimentation in Lake Ohrid (Albania/Macedonia). *Biogeosciences*, 7(10), 3333–3342. <https://doi.org/10.5194/bg-7-3333-2010>
- Vollmer, M. K., Weiss, R. F., Schlosser, P., & Williams, R. T. (2002). Deep-water renewal in Lake Issyk-Kul. *Geophysical Research Letters*, 29(8), 1241–1244. <https://doi.org/10.1029/2002GL014763>
- Wang, J., Wu, J., Zhan, S., & Zhou, J. (2021). Records of hydrological change and environmental disasters in sediments from deep Lake Issyk-Kul. *Hydrological Processes*, 35(4), e14136. <https://doi.org/10.1002/hyp.14136>
- Wang, M., Li, X., Liang, J., Zhang, W., & Hou, J. (2016). Progress in the studies of long chain unsaturated alkenones in Tibetan Plateau lakes (in Chinese). *Quaternary Sciences*, 36(4), 1002–1014. <https://doi.org/10.11928/j.issn.1001-7410.2016.04.21>
- Weber, Y., De Jonge, C., Rijpstra, W. I. C., Hopmans, E. C., Stadnitskaia, A., Schubert, C. J., et al. (2015). Identification and carbon isotope composition of a novel branched GDGT isomer in lake sediments: Evidence for lacustrine branched GDGT production. *Geochimica et Cosmochimica Acta*, 154, 118–129. <https://doi.org/10.1016/j.gca.2015.01.032>
- Weber, Y., Sinnighe Damsté, J. S., Zopfi, J., De Jonge, C., Gilli, A., Schubert, C. J., et al. (2018). Redox-dependent niche differentiation provides evidence for multiple bacterial sources of glycerol tetraether lipids in lakes. *Proceedings of the National Academy of Sciences of the United States of America*, 115(43), 10926–10931. <https://doi.org/10.1073/pnas.1805186115>
- Wennrich, V., Francke, A., Dehnert, A., Juschus, O., Leipe, T., Vogt, C., et al. (2013). Modern sedimentation patterns in Lake El'gygytyn, NE Russia, derived from surface sediment and inlet streams samples. *Climate of the Past*, 9(1), 135–148. <https://doi.org/10.5194/cp-9-135-2013>
- Wessel, P., Luis, J. F., Uieda, L., Scharroo, R., Wobbe, F., Smith, W. H. F., et al. (2019). The generic mapping tools version 6. *Geochemistry, Geophysics, Geosystems*, 20, 5556–5564. <https://doi.org/10.1029/2019GC008515>
- Zavialov, P. O., Izhitskiy, A. S., Kirillin, G. B., Khan, V. M., Konovalov, B. V., Makkaveev, P. N., et al. (2018). New profiling and mooring records help to assess variability of Lake Issyk-Kul and reveal unknown features of its thermohaline structure. *Hydrology and Earth System Science*, 22(12), 6279–6295. <https://doi.org/10.5194/hess-22-6279-2018>
- Zavialov, P. O., Izhitskiy, A. S., Kirillin, G. B., Rezvov, V. Y., Alymkulov, S. A., Zhumaliev, K. M., et al. (2020). Features of thermohaline structure and circulation in Lake Issyk-Kul. *Oceanology*, 60(3), 297–307. <https://doi.org/10.1134/S0001437020020137>
- Zhang, H., Wu, J., Li, Q., & Jin, M. (2021). A ~300-year record of environmental changes in Lake Issyk-Kul, Central Asia, inferred from lipid biomarkers in sediments. *Limnologia*, 90, 125909. <https://doi.org/10.1016/j.limno.2021.125909>
- Zhang, Y., Wang, N., Yang, X., & Mao, Z. (2022). The dynamic changes of Lake Issyk-Kul from 1958 to 2020 based on multi-source satellite data. *Remote Sensing*, 14(7), 1575. <https://doi.org/10.3390/rs14071575>
- Zubovich, A. V., Wang, X.-q., Scherba, Y. G., Schelochkov, G. G., Reilinger, R., Reigber, C., et al. (2010). GPS velocity field for the Tien Shan and surrounding regions. *Tectonics*, 29(6), TC6014. <https://doi.org/10.1029/2010TC002772>